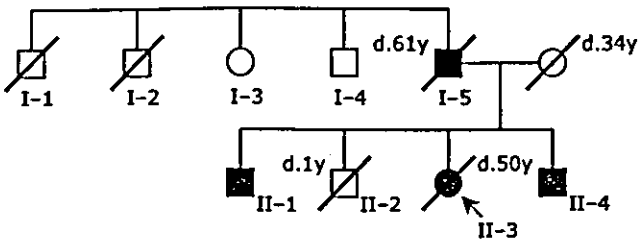

Fig. 1 Family tree of the pedigree. The present case is shown by an *arrow*. Genomic analysis for PRNP was carried out for cases I-5, II-1, 3 and 4. Those patients who developed GSS disease are depicted by a *closed symbol*, while those who have/had PRNP P102L mutations are depicted by a *gray* or *closed symbol*, along with their age at death (years old) (*PRNP* prion protein gene, *GSS* Gerstmann-Sträussler-Scheinker)

were observed in the cerebellar cortices, cerebral cortices and thalamus, although neuronal loss and reactive gliosis were visibly mild. The findings revealed that he was suffering from GSS disease.

No apparent neurological or psychiatric information was available for other relatives. Genomic analysis for PRNP was performed for the current case, her father, and her siblings, and it was revealed that her two brothers II-1 and II-4, her father (patient I-5), and she herself all carried the same genotype of a proline-to-leucine mutation at codon 102 of PRNP and a methionine homozygosity at polymorphic codon 129.

Materials and methods

The autopsied brain was immersion-fixed in 10% formalin and tissue blocks were paraffin-embedded. Another case of GSS with P102L-129 M/M mutation was examined as a control. Hematoxylin and eosin (H-E) stain, Klüver-Barrera (KB) stain and periodic acid-Schiff (PAS) stain were performed on 7-μm-thick sections. Immunohistochemical analyses were performed by a standard indirect immunoperoxidase method for PrP (3F4, Senetek, USA), glial fibrillary acidic protein (GFAP) (G-A-5, Roche, Switzerland), S-100 protein (Novocastra, UK), CD68 (KP1, Dako, Denmark), ubiquitin (Dako, Denmark) and β-amyloid (6F/3D, Dako, Denmark). Sections were pretreated with hydrolytic autoclaving for PrP detection, with citrate-buffered autoclaving for CD68, and with 98% formic acid for β-amyloid. For electron microscopic study of astrocytic inclusion bodies, formalin-fixed tissue blocks of the medial frontal cortex were cut into small pieces. The samples were postfixed in 1% osmium tetroxide, dehydrated through alcohol and propylene oxide, and then embedded in Epon (E. Fullam, USA). Thereafter, ultrathin sections were stained with uranyl acetate and lead citrate, and they were observed under an electron microscope (JEM-100CX, JEOL, Japan).

Results

The post-fixation brain weight was 1,380 g. Although no diffuse atrophy was observed anywhere in the brain, the left inferior frontal gyrus was locally depressed macroscopically. Coronal slices of the cerebrum showed that the left lateral ventricle appeared to be slightly larger than the right side (Fig. 2). Histopathologically, neither neuronal loss nor spongiform change was found anywhere in the brain (Fig. 3A). There were no obvious white matter lesions around the relatively dilated lateral ventricle and no abnormalities in the lamellar arrangement of neurons in the depressed cortical area. Neither astrocytic nor microglial gliosis was demonstrated in the brain by immunohistochemistry for GFAP (Fig. 3C) or CD68 (data not shown), respectively. Immunohistochemistry for PrP failed to detect abnormal PrP deposition anywhere in the brain (Fig. 3E).

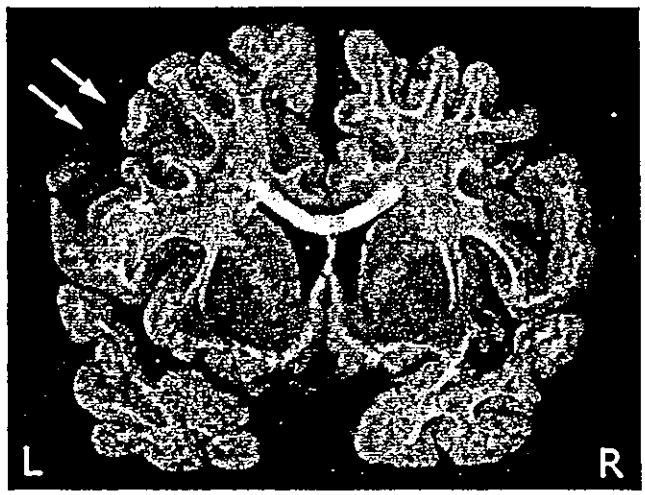

Fig. 2 Coronal section at the caudate-putamen level. The left lateral ventricle is somewhat larger than the right side and left inferior frontal gyrus in this section is depressed (*arrows*)

Aside from GSS-specific pathology, astrocytic cytoplasmic inclusion bodies adjacent to the nuclei were observed, particularly in the superficial layers of the medial frontal cortex and the occipital cortex. The inclusion bodies were amorphous and were eosinophilic by H-E stain (Fig. 3A, inset) and blue-colored by KB stain (Fig. 4A), but they were negative for PAS stain and for the immunostains of GFAP, ubiquitin, PrP and β-amyloid (data not shown). Immunohistochemistry for S-100 protein revealed that the inclusion bodies were negative for S-100 protein but were located within the S-100 protein-positive astrocytes (Fig. 4B). Electron microscopic study showed that the inclusion bodies consisted of non-fibrillar, osmiophilic coarse granular deposits adjacent to the nuclei, with no clear nucleolus (Fig. 4C).

Discussion

We have presented a pre-clinical case with PRNP P102L mutation in a patient who lacked GSS-specific pathological features, even at an age when the clinical manifestations of GSS can readily occur. Although it is impossible to predict when this patient would have developed the disease of GSS, the onset age of P102L-associated GSS is roughly restricted to around the sixth decade. The age at

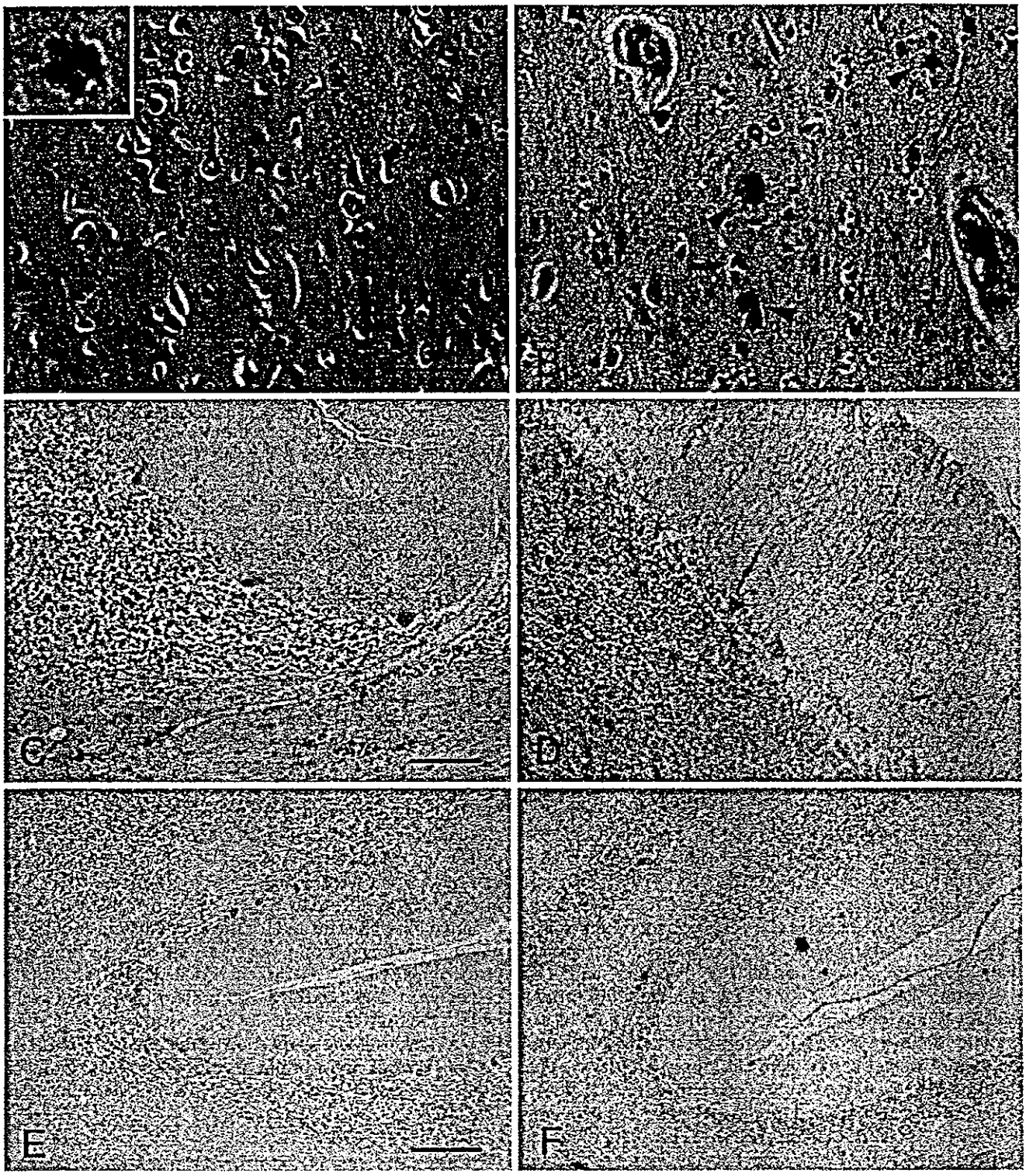

Fig. 3 Neuropathological features of the present case (**A**, **C**, **E**) and a typical GSS case (PRNP P102L-129 M/M, disease onset at 58 years old, with a 7-year disease duration) as a control (**B**, **D**, **F**). **A**, **B** Frontal cerebral cortex, H-E stain. Neither neuronal loss nor spongiform change is evident in this case. Eosinophilic astrocytic inclusion bodies can be frequently seen (**A**, *inset*). Note that the typical GSS case shows numerous kuru-type plaques (**B**, *arrowheads*). **C**, **D** Cerebellum, immunohistochemistry for GFAP. Reactive astrocytosis is absent in this case. **E**, **F** Cerebellum, immunohistochemistry for PrP. No PrP deposition is visible in this case (*GFAP* glial fibrillary acidic protein, *PrP* prion protein). *Bars* **A**, **B** 50 μm; **C**, **D** 100 μm; **E**, **F** 200 μm

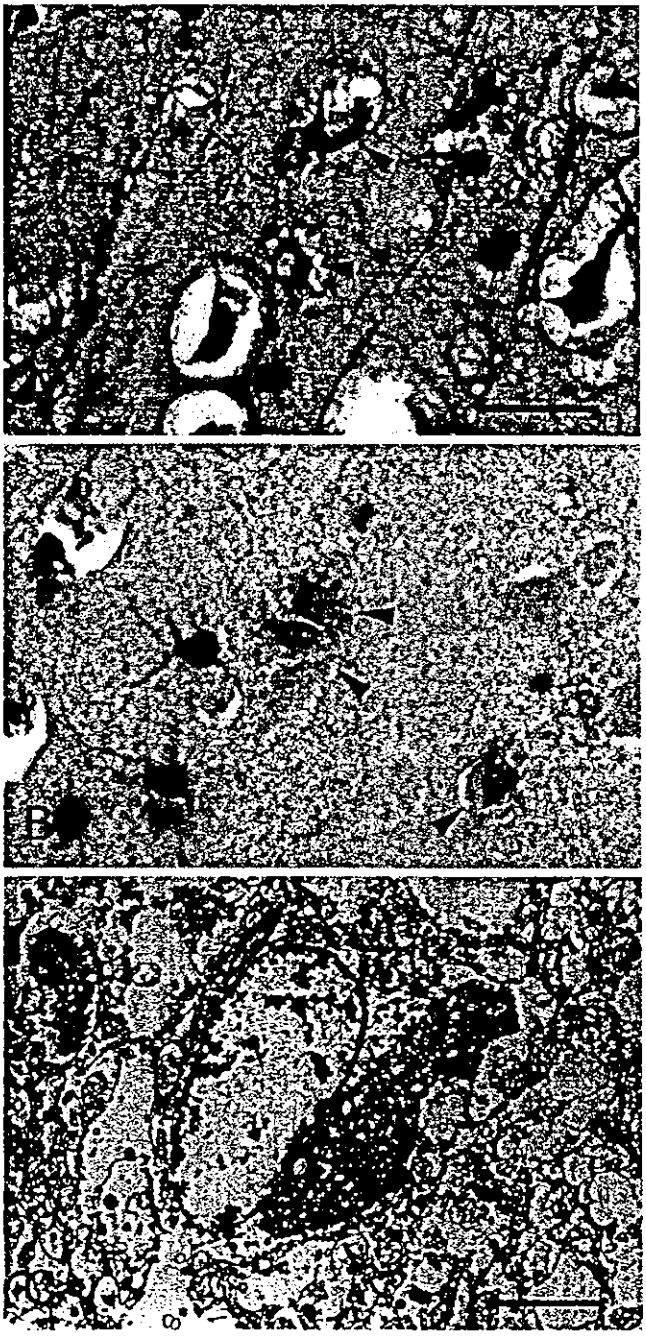

Fig. 4 Histological profile of astrocytic inclusion bodies. A K-B stain. Inclusion bodies (*arrowheads*) are stained blue with Luxol-fast blue. B Immunohistochemistry for S-100 protein. Inclusion bodies (*arrowheads*) are located in the S-100 protein-positive astrocytes, but are immunonegative for S-100 protein themselves. C Electron micrograph. Non-fibrillar, osmiophilic coarse granular inclusion adjacent to the nucleus can be observed. *Bars* A, B 25 μm; C 3 μm

onset in the case of her father was 53 years, while the average age at onset of the cases with P102L-GSS undergoing autopsy in our laboratory (n=10) is 55.7±7.3 years old (Table 1). Taken together with the data of almost 100% disease penetrance in P102L-associated GSS [11], it is interesting that individuals with the mutation responsible for

Table 1 Clinicopathological profiles (*GSS* Gerstmann-Sträussler-Scheinker, PrP prion protein)

	Present case	Patient's father	GSS in our lab (n=10)
Age of onset (years)	50	53	55.7±7.3
Clinical duration (years)	0	8	4.8±2.3
Brain weight (g)	1.380	1.170	966.0±145.5
PrP deposition pattern	Absent	Plaque	Plaque (47.5%) Plaque+diffuse (62.5%; n=8)

GSS have no PrP deposition in the brain in the pre-clinical or non-clinical stage, even at an age close to the average age for disease onset. Thus, it could be estimated that GSS-specific pathology develops within a decade. Biochemical analysis of PrP was not performed because we could not obtain fresh frozen material. Even though immunoblotting assay is useful for verification of protease-resistant PrP (PrP^{res}), it could be certain that immunohistochemistry is no less sensitive for PrP detection than immunoblotting, even if undertaken with sodium phosphotungstic acid precipitation of PrP^{res}. In Alzheimer's disease or in the condition of physiological aging, either β-amyloid deposition or neurofibrillary tangle deposition begins in the brain long before disease manifestation occurs, with manifestation sometimes even failing to occur over a full life span [1, 9]. The situation of the development of GSS pathology is very different from that of Alzheimer's disease. However, the current case is quite a unique case, and it would be necessary to study a larger series of PRNP-P102L cases with non-GSS-associated causes of death to draw any firm conclusions.

The case reported here showed the clinical symptoms of obvious schizophrenia, but this could not have been associated with PRNP P102L mutation because there was no GSS-specific pathology in the brain. Tsai et al. [13] reported that PRNP mutation is not associated with schizophrenia, and the fact that the onset of schizophrenia in this case was much earlier than the appearance of GSS-associated pathology reduces the possibility of a relation between P102L mutation and schizophrenia. Several candidates for the pathological changes seen in schizophrenia have been reported (reviewed in [4, 10]), but no such changes were detected in this case, except for mild hemilateral ventricular dilatation associated with an ipsilateral inferior frontal gyral depression. However, it remains controversial as to whether these changes are in fact specific to schizophrenia.

Astrocytic cytoplasmic inclusions in this case are similar to those previously reported in a case with brain malformation (20-year-old patient with micropolygyria and severe physical and mental retardation, who died of pneumonia after repeated bronchial infections) [6, 8] in respect of morphology, electron microscopy and immunohistochemical findings, except that immunoreactivity for S-100 protein was positive in the previously reported case, but was negative in the present case. We have experienced the

same inclusions in a case with cerebral hemorrhage in some regions not affected by hemorrhage (unpublished data, 82-year-old patient with left thalamic hemorrhage and intraventricular rupture, whose disease duration was 13 days). It can therefore be assumed that these inclusion bodies are not specific to either GSS or schizophrenia.

Acknowledgements We thank Ms. K. Hatanaka for her excellent technical assistance. This study was supported partly by a grant to Dr. K. Doh-ura from the Ministry of Health, Labour and Welfare, Japan. Part of this study was carried out at the Morphology Core, Graduate School of Medical Sciences, Kyushu University. The English used in this manuscript was revised by Miss K. Miller (Royal English Language Centre, Fukuoka, Japan).

References

1. Braak H, Braak E (1997) Frequency of stages of Alzheimer-related lesions in different age categories. Neurobiol Aging 18: 351–357
2. Bugiani, O, Giaccone G, Piccardo P, Morbin M, Tagliavini F, Ghetti B. (2000) Neuropathology of Gerstmann-Straussler-Scheinker disease. Microsc Res Tech 50:10–15
3. Doh-ura K, Tateishi J, Sasaki H, Kitamoto T, Sakaki Y (1989) Pro→leu change at position 102 of prion protein is the most common but not the sole mutation related to Gerstmann-Straussler syndrome. Biochem Biophys Res Commun 163:974–979
4. Halliday GM (2001) A review of the neuropathology of schizophrenia. Clin Exp Pharmacol Physiol 28:64–65
5. Hsiao K, Baker HF, Crow TJ, Poulter M, Owen F, Terwilliger JD, Westaway D, Ott J, Prusiner SB (1989) Linkage of a prion protein missense variant to Gerstmann-Straussler syndrome. Nature 338:342–345
6. Kato S, Hirano A, Umahara T, Herz F, Shioda K, Minagawa M (1992) Immunohistochemical studies on the new type of astrocytic inclusions identified in a patient with brain malformation. Acta Neuropathol 84:449–452
7. Kretzschmar HA, Honold G, Seitelberger F, Feucht M, Wessely P, Mehraein P, Budka H (1991) Prion protein mutation in family first reported by Gerstmann, Straussler, and Scheinker. Lancet 337:1160
8. Minagawa M, Shioda K, Shimizu Y, Isshiki T (1992) Inclusion bodies in cerebral cortical astrocytes: a new change of astrocytes. Acta Neuropathol 84:113–116
9. Ogomori K, Kitamoto T, Tateishi J, Sato Y, Tashima T (1988) Aging and cerebral amyloid: early detection of amyloid in the human brain using biochemical extraction and immunostain. J Gerontol 43:B157–162
10. Powers RE (1999) The neuropathology of schizophrenia. J Neuropathol Exp Neurol 58:679–690
11. Prusiner SB (1994) Inherited prion diseases. Proc Natl Acad Sci USA 91:4611–4614
12. Tateishi J, Kitamoto T, Hashiguchi H, Shii H (1988) Gerstmann-Straussler-Scheinker disease: immunohistological and experimental studies. Ann Neurol 24:35–40
13. Tsai MT, Su YC, Chen YH, Chen CH (2001) Lack of evidence to support the association of the human prion gene with schizophrenia. Mol Psychiatry 6:74–78

0023-6837/03/8312-1751$03.00/0
LABORATORY INVESTIGATION

Vol. 83, No. 12, p. 1751, 2003
Printed in U.S.A.

A Novel Tool for Detecting Amyloid Deposits in Systemic Amyloidosis In Vitro and In Vivo

Yukio Ando, Katsuki Haraoka, Hisayasu Terazaki, Yutaka Tanoue, Kensuke Ishikawa, Shoichi Katsuragi, Masaaki Nakamura, Xuguo Sun, Kazuko Nakagawa, Kazumi Sasamoto, Kazuhiro Takesako, Takashi Ishizaki, Yutaka Sasaki, and Katsumi Doh-ura

Department of Laboratory Medicine (YA, MN, XS) and Department of Gastroenterology and Hepatology (KH, HT, YS), Kumamoto University School of Medicine, Kumamoto, and Department of Pharmacology and Therapeutics (YT, KN, TI), Graduate School of Clinical Pharmacy, Kumamoto University, Kumamoto, and Department of Neuropathology (KI), Neurological Institute, Graduate School of Medical Sciences, Kyushu University, Fukuoka, Division of Prion Protein Biology (KD), Department of Prion Research, Tohoku University Graduate School of Medicine, Sendai, and Department of Psychiatry (SK), Kikuchi National Hospital, Koshi-machi, Kikuchi-Gun, Kumamoto, and Dojin Chemical Company (KS, KT), Mashiki, Kamimashiki, Kumamoto, Japan

SUMMARY: We synthesized (*trans,trans*)-1-bromo-2,5-bis-(3-hydroxycarbonyl-4-hydroxy)styrylbenzene (BSB) and used this compound to detect amyloid fibrils in autopsy and biopsy samples from patients with localized amyloidosis, such as familial prion disease, and systemic amyloidosis, such as familial amyloidotic polyneuropathy, amyloid A (AA) amyloidosis, light chain (AL) amyloidosis, and dialysis-related amyloidosis. BSB showed reactions in all Congo red-positive and immunoreactive regions of the samples examined in the study, and some amyloid fibrils in the tissues could be detected more precisely with BSB than with the other methods. In the mouse model of AA amyloidosis, injected BSB reacted with amyloid in all regions in the serial sections in which Congo red staining was positive. A highly sensitive 27-MHz quartz crystal microbalance analysis revealed that BSB showed a significant affinity for amyloid fibrils purified from familial amyloidotic polyneuropathy and dialysis-related amyloidosis samples and suppressed formation of transthyretin amyloid in vitro. These results suggest that BSB may become a valuable tool for detection of amyloid deposits in amyloidosis and of the mechanism of amyloid formation. (*Lab Invest 2003, 83:1751–1759*).

Progress in molecular genetics and biochemical methodologies has led to the identification of various types of amyloidosis and their amyloidogenic precursor proteins (Benson, 1995; Ikeda et al, 2002; Saraiva, 2001; Tan and Pepys, 1994; Tan et al, 1995). Thus far, 24 different amyloidogenic proteins have been identified; however, the mechanism of amyloid formation has been elucidated in only several types of amyloidosis (Ando et al, 2002; Benson et al, 1993; Benson and Uemichi, 1996; Pepys et al, 1993; Soutar et al, 1992; Westermark et al, 2002). One of the most important steps in the diagnosis of the specific type of amyloidosis is detection of amyloid deposits in tissues. It is not easy to predict the presence of these amyloid deposits on the basis of patients' clinical manifestations, that is, without histopathologic materials. Thus, amyloidosis is sometimes diagnosed after the death of the patients (Ishihara et al, 1989).

In systemic amyloidosis, such as familial amyloidotic polyneuropathy (FAP), AA amyloidosis, AL amyloidosis, and dialysis-related amyloidosis (DRA), biopsy samples are often obtained from the gastrointestinal tract and abdominal fat to make the diagnosis (Guy and Jones, 2001; Kaplan et al, 1999; Masouye, 1997) because amyloid deposits are usually found in these tissues at the early stage of the disease. However, in certain cases it is sometimes difficult to make the diagnosis using only the biopsy samples, because the pattern of amyloid deposition in the body varies in each individual (Ishihara et al, 1989). In addition, biopsy for diagnostic purposes cannot usually be performed in patients with localized amyloidosis, such as in Alzheimer's disease and endocrine amyloidosis (Westermark and Westermark, 2000). Diagnosis at the early stage of amyloidosis might be possible if a tool were available that incorporated real-time amyloid monitoring, such as radioisotope-labeled scintigraphy (Hawkins et al, 1990; Pulle et al, 2002).

DOI: 10.1097/01.LAB.0000101701.87433.C5

Received February 20, 2003.

YA and KH contributed equally to the study. This work was supported by grants from the Amyloidosis Research Committee and the Pathogenesis, Therapy of Hereditary Neuropathy Research Committee, Surveys and Research on Specific Disease, the Ministry of Health and Welfare of Japan, Charitable Trust Clinical Pathology Research Foundation of Japan, and Grants-in-Aid for Scientific Research (C) 13670655 and (B) 15390275 from the Ministry of Education, Science, Sports and Culture of Japan.

Address reprint requests to: Dr. Y. Ando, Department of Laboratory Medicine, Kumamoto University School of Medicine, Japan.

Among several histopathologic methods with stains such as Congo red, Pagoda red, and thioflavin S, Congo red staining is one of the most popular detection methods of amyloid deposits in tissues (Puchtler and Sweat, 1965; Westermark et al, 1999). Congo red is a hydrophilic chemical agent that binds to amyloid fibrils in vitro (Benditt et al, 1970; Westermark et al, 1999). Apple green birefringence under polarized light after Congo red staining is the most reliable evidence of the presence of amyloid fibrils in biopsy and/or autopsy materials from patients with amyloidosis (Sipe and Cohen, 2000; Westermark et al, 1999), although Congo red-stained histochemical sections are not always easy to interpret. However, the Congo red stain cannot be used for in vivo studies because it has toxic effects in the human body (Bi et al, 1992; Case et al, 1954; Giger et al, 1974; Giger and Zbinden, 1974; Kennelly et al, 1984; Zenser et al, 1998). Chrysamine G, a Congo red derivative with a similar molecular structure used for the same purpose as Congo red, has the same limitations (Dezutter et al, 1999, 2001a; Klunk et al, 1995, 1998). To overcome these problems, we must have a new tool for examination of amyloid deposition in tissues.

(*trans,trans*)-1-bromo-2,5-bis-(3-hydroxycarbonyl-4-hydroxy)styrylbenzene (BSB), which has been found to bind to amyloid plaques in postmortem samples of brains from patients with Alzheimer's disease, is also a Congo red derivative and has been the focus of recent attention (Klunk et al, 1994; Schmidt et al, 2001; Skovronsky et al, 2000; Zhuang et al, 2001a, 2001b). Because this compound is lipophilic, it can traverse the blood-brain barrier, and it binds to amyloid fibrils in the brain when it is injected intravenously into transgenic mice with Alzheimer's disease (Skovronsky et al, 2000). Moreover, this compound can detect cell inclusion bodies derived from α-synclein (Schmidt et al, 2001). However, no studies have addressed the question of whether the compound could become a useful tool for detection of amyloid deposits in systemic amyloidosis. Various plasma proteins in the systemic circulation may disturb the binding of BSB to amyloid fibrils in tissues.

In this study, we carefully checked the reactivity of BSB with amyloid fibrils found in various types of systemic amyloidosis and a familial type of prion disease. To determine the usefulness of the compound in vivo, we also examined BSB reactivity in amyloid deposits in mice in which AA amyloidosis had been induced. In addition, we investigated the affinity of BSB for amyloid fibrils and the inhibitory effect of BSB on formation of transthyretin (TTR) amyloid fibrils in vitro by means of a highly sensitive 27-MHz quartz crystal microbalance (QCM) (Matsuno et al, 2001; Okahata et al, 1998) and electron microscopy, respectively.

Results

BSB Reactivity with Amyloid in Deposits in Various Types of Amyloidosis

BSB reacted with amyloid in deposits in familial prion disease and in various systemic amyloidoses such as FAP, AA, AL, and DRA (Fig. 1). Except for reactions in familial prion disease, BSB reactions were noted in lesions in which the antibodies also showed a positive reaction. Compared with the sensitivity of Congo red staining, the sensitivity of BSB was more precise, with a greater contrast in the BSB-positive areas in the tissues.

BSB Reactivity with Amyloid in Deposits in AA Amyloidosis in Vivo

We injected BSB into mice in which AA amyloidosis had been induced. We examined spleen samples and found that 24 hours after the injection of BSB into the mice, BSB-positive lesions were not obviously detected. However, 48 hours after the injection, BSB-positive lesions were clearly detected in both tissues. BSB reactions were seen in all lesions in the serial sections in which positive Congo red staining was confirmed under polarized light. Figure 2 shows amyloid deposits stained by BSB in vivo.

Affinity of BSB or Congo Red for Amyloid Fibrils

The frequency of the QCM responding to BSB decreased over time, which indicated that BSB had significant affinity for the amyloid fibrils purified from intestinal DRA and vitreous FAP samples. However, neither wild-type TTR nor the variant TTR showed any affinity for BSB (Fig. 3A). In a comparison of amyloid fibrils in the FAP and DRA samples, BSB showed a stronger affinity for DRA amyloid fibrils than for FAP amyloid fibrils.

BSB exhibited a strong affinity for amyloid fibrils; the amount of BSB bound to the amyloid was greater than the amount of Congo red bound to amyloid ($M[BSB]_{max}$: 266 ng/cm^2, and $M[Congo\ red]^{max}$: 157 ng/cm^2), whereas the affinity of BSB for amyloid was weaker than that of Congo red (BSB: $K_A = 5.66 \times 10^5$/M, $K_D = 1.76$ μM; Congo red: $K_A = 2.17 \times 10^6$/M, $K_D = 0.46$ μM) (Fig. 3, B and C).

Inhibitory Effect of BSB on Amyloid Formation

Electron microscopic analysis of the morphology of incubated TTR revealed that the fibrils in the absence of BSB were straight, nonbranched filament structures with helical periodicity and close to an authentic structure of amyloid fibrils (Fig. 4A). In comparison, the fibrils in the presence of BSB had irregularly short-curled shapes, and the morphology of these fibrils was clearly distinct from that of typical amyloid fibrils (Fig. 4B).

Discussion

We demonstrated herein that BSB clearly reacted with amyloid in all amyloid deposits in the samples examined both in vitro and in vivo. Obvious BSB reactions with amyloid were noted, and the sensitivity of BSB for amyloid was better than that shown by Congo red. Although we could not find any Congo red-negative or precursor protein aggregate-positive lesions, so-

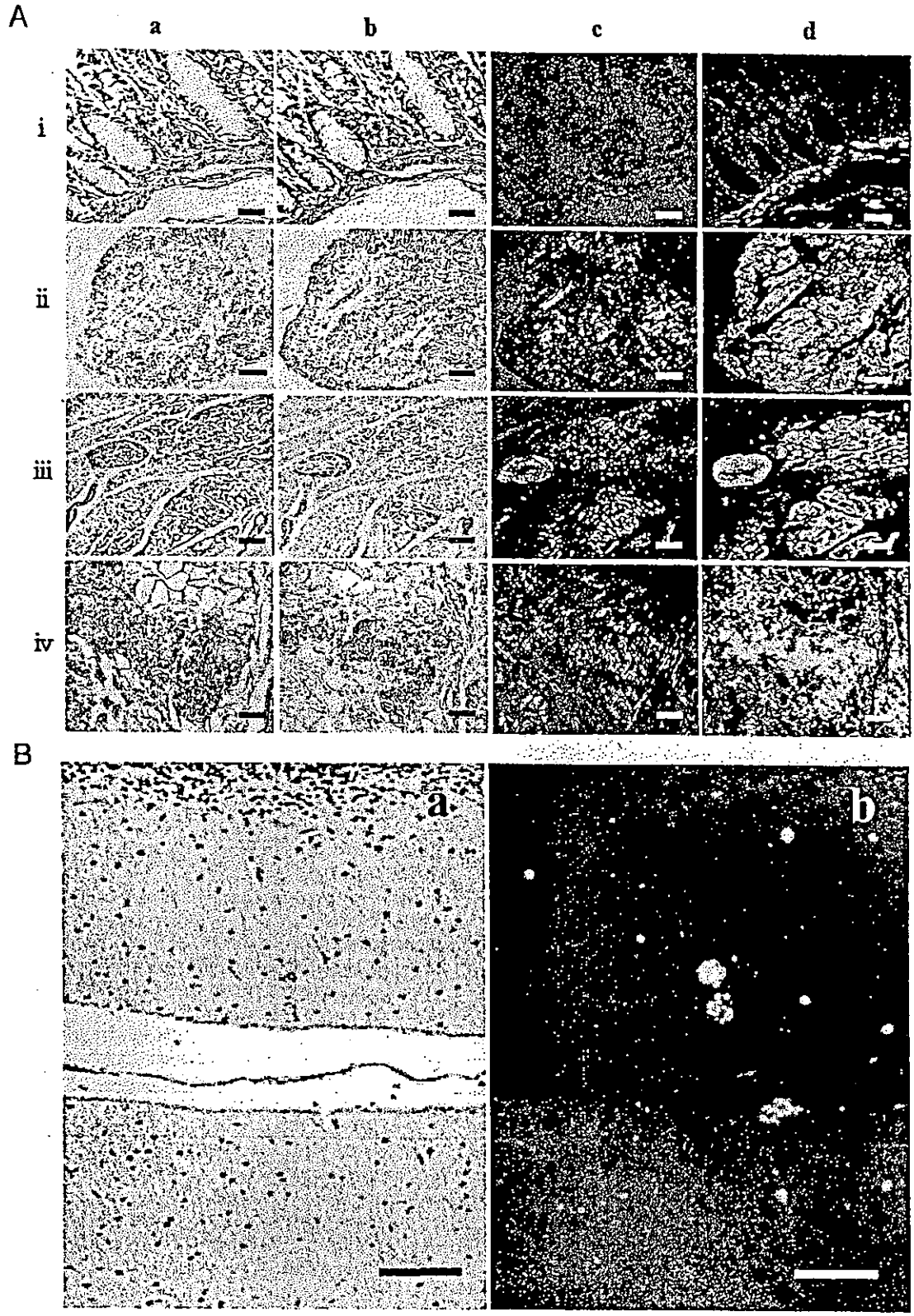

Figure 1.

(*trans,trans*)-1-bromo-2,5-bis-(3-hydroxycarbonyl-4-hydroxy)styrylbenzene (BSB) reactivity in various kinds of amyloidosis. Paraffin-embedded samples from patients with systemic amyloidosis (A) and familial prion disease (B). A: a, Immunohistochemical staining for amyloidogenic proteins with antibodies as described in the text. b and c, Staining with Congo red with hematoxylin and polarized light photographs, respectively. d, BSB staining. *Row i:* familial amyloidotic polyneuropathy (FAP), scale bars = 10 μm; *row ii:* dialysis-related amyloidosis (DRA), scale bars = 50 μm; *row iii:* AA amyloidosis, scale bars = 100 μm; *row iv:* AL amyloidosis, scale bars = 200 μm. B: a, Staining with Congo red with hematoxylin of familial type of prion disease; b, its BSB staining. Scale bars = 100 μm.

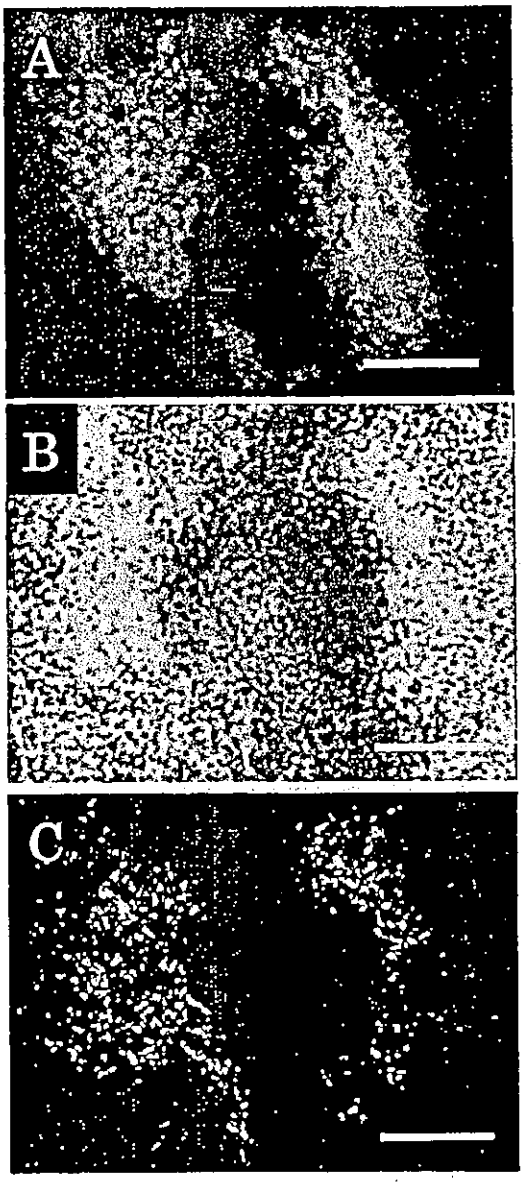

Figure 2.
BSB reactivity with amyloid in vivo. A, Microscopy of a spleen section from a BSB-injected mouse with AA amyloidosis. Fluorescence of BSB was observed under UV light. B and C, Staining with Congo red with hematoxylin and polarized light photograph, respectively. Scale bars = 150 μm.

called preamyloid state lesions, the dye might react with such lesions. When the color of the Congo red staining is close to the original color of tissues examined (Fig. 1B) or the amount of amyloid is small or scarce, we sometimes could not distinguish the presence or absence of amyloid deposition. In contrast, BSB examined under UV light had a whitish blue color, so we could clearly differentiate the amyloid deposits from the nonamyloid-containing tissues.

Comparison of BSB reactivity with staining of antibodies for amyloidogenic proteins revealed the same staining patterns for BSB and antibodies. BSB also reacted with amyloid in deposits in a brain sample from a patient with familial prion disease, a disease in which amyloid plaques were found in the brain, similar to amyloid deposits in the brain found in Alzheimer's disease (Skovronsky et al, 2000).

However, in samples from patients with a nonfamilial type of prion disease, which shows no amyloid plaques in the brain, no BSB-positive lesions were obtained (data not shown). These results suggest that BSB staining is useful for detecting amyloid clusters predominantly in systemic amyloidotic samples.

In systemic amyloidoses such as FAP, AA, AL, and DRA, most of the diagnostic methods are invasive (Guy and Jones, 2001; Ishihara et al, 1989; Kaplan et al, 1999; Masouye, 1997), with biopsy of the gastrointestinal system, abdominal fat, or sural nerves often used. However, amyloid deposition is not uniform in all forms of systemic amyloidosis (Ishihara et al, 1989; Tan and Pepys, 1994). Sometimes, no amyloid deposits can be observed in biopsy materials (Ishihara et al, 1989), although it is suspected that the disease process of amyloidosis has already started. In vivo real-time monitoring methods (Hawkins et al, 1990; Puille et al, 2002) would be beneficial for making the diagnosis of amyloidosis.

Serum amyloid P component (SAP) scintigraphy (Hachulla et al, 1994, 1996; Hawkins et al, 1990; Rydh et al, 1998; Salle et al, 1993) has been used to detect amyloid deposits in patients, because SAP is commonly found in amyloid deposits in all types of amyloidosis. Although SAP scintigraphy has made an invaluable contribution to diagnosis and is to date the only safe method, a nonspecific SAP reaction in the liver and kidneys is sometimes noted (Hawkins et al, 1990; Puille et al, 2002). Moreover, purification of SAP protein is difficult, because the molecule easily binds to various plasma and tissue proteins (Hawkins et al, 1990; Tan and Pepys, 1994). Scintigraphy with technetium-99m 3,3-diphosphono-1,2-propanodicarboxylic acid (^{99m}Tc-DPD) may be useful, but it has revealed amyloid deposits of only FAP (Puille et al, 2002). In addition, scintigraphy with ^{99m}Tc-labeled monoamide-monoaminedithiol chrysamine G was useful in chickens with amyloid arthropathy, but no data on human amyloidosis or other types of amyloidosis in animal models in vivo were provided (Dezutter et al, 2001b). In addition, the labeling of compounds to ^{99m}Tc for imaging must be conducted under conditions that use covalent chelating agents so that no separation of the label from the nuclide occurs in vivo (Moran, 1999).

The possibility of using BSB for scintigraphy in the brain has been proposed (Skovronsky et al, 2000). As demonstrated in Figure 2, after intravenous BSB injection into mice, BSB reactivity showed a significant colocalization with amyloid deposits stained by Congo red. In contrast, we found no accumulation of Congo red in amyloid deposits after Congo red injection into mice, although most of the mice died within several hours (data not shown). In addition, it has been well documented that Congo red has toxic effects, especially on platelets (Giger et al, 1974; Giger and Zbinden, 1974). Moreover, Congo red as well as chrysamine G is classified into a group of azo dyes that contain a benzidine structure (Kennelly et al,

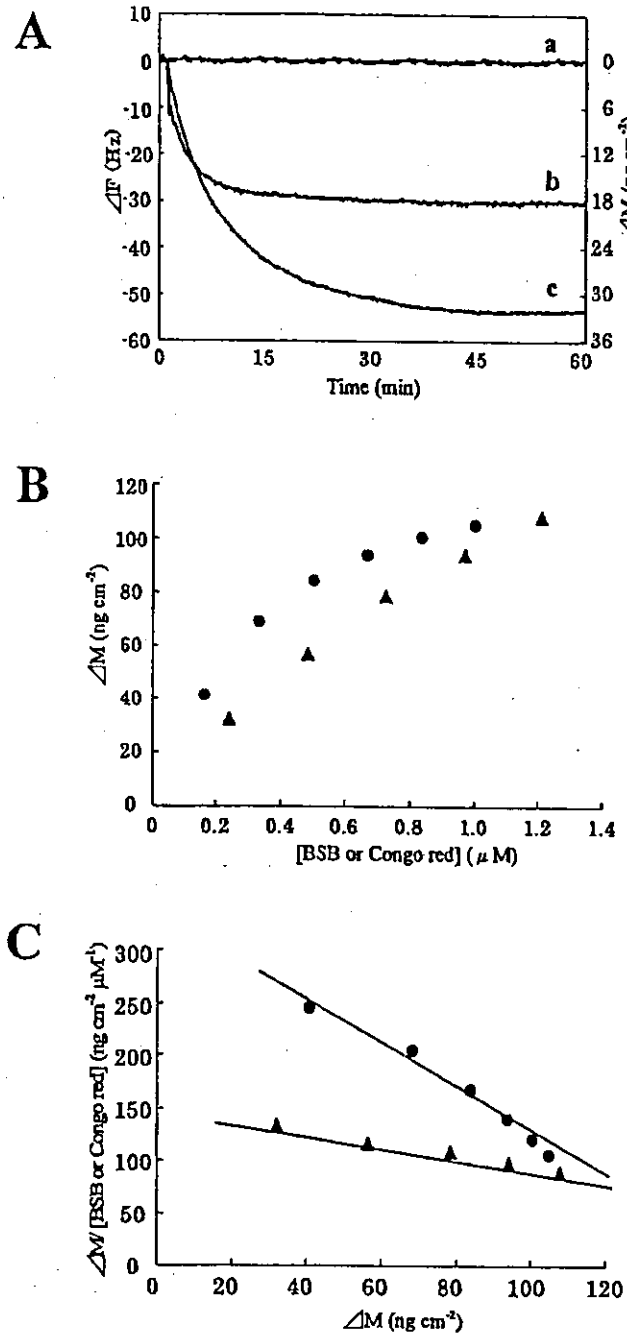

Figure 3.

A, Affinity of BSB for FAP or DRA amyloid fibrils and for transthyretin (TTR). Time courses of frequency changes (ΔF) of the quartz crystal microbalance (QCM) directory immobilized with FAP or DRA amyloid fibrils or with TTR were demonstrated. BSB dissolved in 10% dimethyl sulfoxide (DMSO) was added into a buffered solution (10 mM Tris-HCl, 10% DMSO, pH 7.4, 25 °C), at a final concentration of 1.45 nmol. Frequency changes (ΔF) of the QCM were converted into QCM binding amount (ΔM) according to the Sauerbrey Equation (ΔF (Hz) = 0.6 ng/cm²) (Sauerbrey, 1959). a, TTR; b, FAP amyloid fibrils; c, DRA amyloid fibrils. B, Binding behavior of DRA amyloid fibrils depending on the concentration of BSB or Congo red. Increasing ΔM by administration of BSB or Congo red into the solution in each time spot (10 mM Tris-HCl, 10% DMSO, pH 7.4, 25 °C) resulted in a typical saturation binding curve [BSB concentrations: 1.45–7.27 nmol in 6 mL (0.24- 1.21 μM); Congo red concentrations: 1.00–6.03 nmol in 6 mL (0.41- 2.46 μM)]. *Closed circles* = Congo red; *closed triangles* = BSB. C, Scatchard plot of affinities of BSB or Congo red for DRA amyloid fibrils

$$\Delta M/[\text{BSB or Congo red}] = \Delta M_{max}/K_D - \Delta M/K_D \quad (1)$$

$$K_A = 1/K_D \quad (2)$$

Scatchard plots of the data in B gave a simple straight line according to Equation 1. Association constants (K_A) and the maximum binding amount (ΔM_{max}) to DRA amyloid fibrils were calculated from the slope and the intercept of the x-axis in the plot, respectively. *Closed circles* = Congo red; *closed triangles* = BSB.

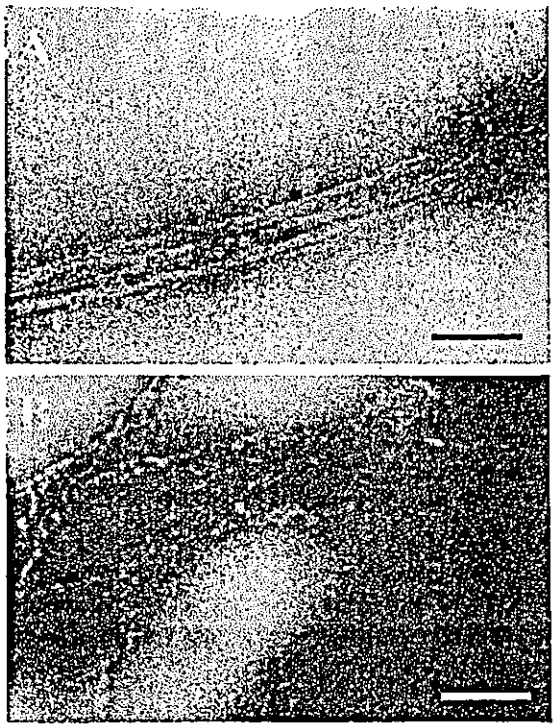

Figure 4.
Inhibitory effect of BSB as assessed by electron microscopy. Electron micrographs of the morphology of incubated wild-type TTR in the absence of BSB (A) and in the presence of BSB (B), as described in "Materials and Methods." Nonbranched helical filament structures were seen in the condition of A, and branched, short-curled fibrillar substances were seen in the condition of B. Scale bars = 30 nm.

1984; Zenser et al, 1998; Zhuang et al, 2001a, 2001b). Compounds possessing the benzidine structure show carcinogenic effects when administered in vivo (Bi et al, 1992; Case et al, 1954). In contrast to Congo red, BSB may be beneficial in scintigraphic studies of systemic amyloidosis in humans, because it has no benzidine structure and can be easily modified at the Br position of the BSB molecule (Zhuang et al, 2001a, 2001b).

Additional effects of BSB—its affinity for amyloid and its inhibition of amyloid formation—were also studied. Figure 3 indicates the affinity of BSB for TTR, FAP amyloid fibrils, or DRA amyloid fibrils. QCM is a new tool for measuring the affinity of a protein for a protein, a protein for a DNA, and/or a protein for a chemical compound (Matsuno et al, 2001; Okahata et al, 1998). Our results confirmed the strong affinity of BSB for amyloid fibrils but not for the amyloidogenic protein. Figure 4 shows an inhibitory effect of BSB on formation of TTR amyloid in vitro. In the presence of BSB, TTR could not become complete fibrils; we observed only immature amyloid fibrils. Recently, the thioflavin T test has been used to evaluate the degree of amyloid formation in vitro (LeVine, 1993). However, we did not analyze the effect of BSB on amyloid formation in vitro as assessed by the thioflavin *t* test because that method examines the competitive inhibition between thioflavin T and BSB (Zhuang et al, 2001a, 2001b), and we are not aware of the true effect of BSB on amyloid formation of the TTR molecule with this method. Therefore, we used electron microscopy for our analysis. Our data suggest that BSB may become a useful tool for suppressing amyloid formation in systemic amyloidosis.

In summary, we have illustrated the usefulness of BSB for detection of amyloid deposits in vitro and in vivo, as well as the therapeutic potential for BSB in amyloidosis. BSB has only recently been developed, so information on its potential effects on the human body is not available. In vivo studies of BSB are definitely required for elucidating its potential validity for the diagnosis and treatment of amyloidosis.

Materials and Methods

Subjects and Materials

For the histopathologic examinations, autopsy samples from 10 patients with FAP (five men and five women; average 34.6 ± 5.8 years old) were included in the study. All patients had a definitive diagnosis of FAP ATTR Val30Met on the basis of clinical findings, amyloid deposits in biopsy specimens, and a positive test for ATTR Val30Met (Terazaki et al, 1999). One patient with AL amyloidosis (a 58-year-old woman), three patients with secondary amyloidosis (two men and one woman; average 48.6 ± 5.6 years old), seven patients with DRA (three men and four women; average 53.4 ± 6.7 years old), and one patient with familial prion disease all had diagnoses based on clinical and histopathologic findings.

Histochemical Analyses

Each tissue sample was obtained at autopsy. Sections were cut 3-μm thick from paraffin-embedded blocks of tissue and were stained with alkaline Congo red. Congo red reactivity was confirmed under polarized light (Puchtler and Sweat, 1965; Westermark et al, 1999). For BSB staining, sections were immersed in 0.01% BSB in 50% EtOH for 30 minutes. Sections were quickly differentiated in saturated Li_2CO_3 and rinsed in 50% EtOH before examination by fluorescence microscopy (Skovronsky et al, 2000). Rabbit anti-human TTR antibody, rabbit anti-human kappa, lambda light chain antibodies, anti-human μ_2-microglobulin antibody, and rabbit anti-human amyloid A component antibody (Dako, Glostrup, Denmark) were used for the immunohistochemical studies. The ABC method was used (Dako) according to the manufacturer's instructions. All chemicals used in histochemical and biochemical studies were of analytical grade.

BSB Synthesis

BSB was synthesized according to the method described by Zhuang et al (2001a, 2001b) with slight modifications. Briefly, the Wittig-Horner-Emmons reaction with 2-methoxy-5-formyl benzoic acid methyl ester and 2-bromo-1,4-bis(diethylphosphonato)xylene provided the coupled product, 1-bromo-2,5-bis(3-

methoxycarbonyl-4-methoxy)styrylbenzene, as a 49% yield. After deprotection with a large excess of BBr_3 in dichloromethane followed by hydrolysis, BSB was obtained at a 20% overall yield, as a yellowish powder. HPLC analysis (Wakosil II 5C18HG) with a 4:1 (v/v) mixture of acetonitrile and 10 mM phosphate buffer (pH 7.0) as an eluent showed 99% purity, as detected at 254 nm. IR (KBr): 3500, 1680 cm^{-1}, FAB-MS: *m/z* 481 (M^+1), and ^{1}H-NMR (300 MHz, DMSO-d_6) spectrum data were in good agreement with results reported by Zhuang et al (2001a, 2001b).

Induction of AA Amyloidosis in Mice

Complete Freund's adjuvant and *Mycobacterium butyricum* were from Difco Laboratories (Detroit, Michigan). AA amyloidosis was induced in C57BL/6J mice according to the method of Hoshii et al (1997). Emulsions of complete Freund's adjuvant with *M. butylicum* were prepared as follows: equal volumes of complete Freund's adjuvant and PBS were added to samples of *M. butylicum* and emulsified in the cold under sterile conditions. Aliquots of 250 μl of emulsion were injected intraperitoneally into the mice.

Injection and In Vivo Characterization of BSB

Four weeks after 250 μl of emulsion was injected into the mice, 200 μl of 0.2% BSB in mouse serum was injected via the tail vein. Six mice were allowed to recover for 24 or 48 hours before they were killed by decapitation, and spleens were removed and frozen. Sections 8- to 10-μm thick were cut by cryostat, dried, and imaged with no additional staining. After sections were imaged, serial sections were stained with Congo red.

Amyloid Formation in Human TTR

Denatured TTR was generated by the procedure of Goldberg et al (1991). To evaluate amyloid fibril formation via partial TTR denaturation, 15 μM TTR was mixed in 50 mM sodium acetate (pH 3.0–4.0) containing 100 mM KCl, with or without 20 μM BSB, and incubated with agitation at 37 °C for 4 weeks.

Affinity of BSB or Congo Red for Amyloid Fibrils

FAP amyloid fibrils were collected by centrifugation from vitrectomized corpus vitreum from patients with FAP. The samples were then washed three times with 1 ml of saline and 1 ml of distilled water, respectively, and were centrifuged (9000 ×*g* for 5 minutes) (Ando et al, 1999). DRA amyloid fibrils were purified from an intestinal sample from a patient as described by Naiki et al (1989). The affinity of BSB or Congo red for amyloid fibrils was examined by using a highly sensitive 27-MHz QCM (Affinix Q; Initium Company, Tokyo, Japan) as described (Matsuno et al, 2001; Okahata et al, 1998). Briefly, 2 μl of 100 μg/ml purified amyloid fibrils, 2 μl of 100 μg/ml purified wild-type TTR, or the variant TTR (ATTR Val30Met) was directly immobilized on a QCM plate, the plate was soaked in 6 ml of a buffered solution [10 mM Tris-HCl, 10% dimethyl sulfoxide (DMSO), pH 7.4] at 25 °C, and the resonance frequency of the QCM was defined as the 0 position after equilibrium. Then, BSB or Congo red solution (dissolved in 10% DMSO) was injected silently into the buffered solution, and time courses of the change in frequency of the QCM responding to BSB or Congo red was recorded. The stability and drift of the 27-MHz QCM frequency in the solution were ± 5 Hz for 12 hours at 25 °C.

Electron Microscopic Analyses

The sample containing the synthesized TTR filaments was centrifuged at 15,000 ×*g* for 90 minutes. Pellets were placed on collodion-coated grids and negatively stained with 2% phosphotungstic acid adjusted to pH 7.4. The specimens were examined under a Hitachi H7000 electron microscope (Hitachi Company, Hitachi, Japan) with an accelerating voltage of 100 kV.

Acknowledgements

We thank the Trustees of the University of Pennsylvania for providing a significant amount of BSB to perform the experiments.

References

Ando Y, Ando E, Ohlsson PI, Olofsson Å, Sandgren O, Suhr O, Terazaki H, Obayashi K, Lundgren E, Ando M, and Negl A (1999). Analysis of transthyretin (TTR) forms of amyloid fibrils from vitreous samples in familial amyloidotic polyneuropathy. (Met30). Amyloid 6:119–123.

Ando Y, Nakamura M, Kai H, Katsuragi S, Terazaki H, Nozawan T, Okuda T, Misumi S, Matsunaga N, Tajiri T, Shoji S, Yamashita T, Haraoka K, Obayashi K, Matsumoto K, Ando M, and Uchino M (2002). A novel localized amyloidosis associated with lactoferrin in the cornea. Lab Invest 82:757–766.

Benditt EP, Eriksen N, and Berglund C (1970). Congo red dichroism with dispersed amyloid fibrils, an extrinsic cotton effect. Proc Natl Acad Sci USA 66:1044–1051.

Benson MD (1995). Amyloidosis. In: Scriver CR, Beaudet AK, Sly WS, and Valle D, editors. The metabolic and molecular bases of inherited disease. New York: McGraw-Hill, 4159–4191.

Benson MD, Liepnieks J, Uemichi T, Wheeler G, and Correa R (1993). Hereditary renal amyloidosis associated with a mutant fibrinogen-chain. Nat Genet 3:252–255.

Benson MD and Uemichi T (1996). Transthyretin amyloidosis. Amyloid 3:44–56.

Bi W, Hayes RB, Feng P, Qi Y, You X, Zhen J, Zhang M, Qu B, Fu Z, Chen M, Co Chien HT, and Blot WJ (1992). Mortality and incidence of bladder cancer in benzidine-exposed workers in China. Am J Ind Med 21:481–489.

Case RAM, Hosker MW, McDonald DB, and Pearson JT (1954). Tumors of the urinary bladder in workmen engaged in the manufacture and use of certain dyestuff intermediates in the British chemical industry. Br J Ind Med 11:75–104.

Dezutter NA, Dom RJ, de Groot TJ, Bormans GM, and Verbruggen AM (1999). ^{99m}Tc-MAMA-chrysamine G, a probe

for beta-amyloid protein of Alzheimer's disease. Eur J Nucl Med 26:1392–1399.

Dezutter NA, Landman WJ, Jager PL, de Groot TJ, Dupont PJ, Tooten PC, Zekarias B, Gruys E, and Verbruggen AM (2001a). Evaluation of ^{99m}Tc-MAMA-chrysamine G as an in vivo probe for amyloidosis. Amyloid 8:202–214.

Dezutter NA, Sciot RM, de Groot TJ, Bormans GM, and Verbruggen AM (2001b). In vitro affinity of ^{99}Tcm-labelled N2S2 conjugates of chrysamine G for amyloid deposits of systemic amyloidosis. Nucl Med Commun 22:553–558.

Giger M, Baumgartner HR, and Zbinden G (1974). Toxicological effects of Evans blue and Congo red on blood platelets. Agents Actions 4:173–180.

Giger M and Zbinden G (1974). Significance of the albumin concentration for the toxic effect of Evans blue and Congo red on thrombocytes. Schweiz Med Wochenschr 104:1376–1377.

Goldberg ME, Rudolph R, and Jaenicke R (1991). A kinetic study of the competition between renaturation and aggregation during the refolding of denatured-reduced 197-egg white lysozyme. Biochemistry 30:2790–2797.

Guy CD and Jones CK (2001). Abdominal fat pad aspiration biopsy for tissue confirmation of systemic amyloidosis: Specificity, positive predictive value, and diagnostic pitfalls. Diagn Cytopathol 24:181–186.

Hachulla E, Deveaux M, Duquesnoy B, and Marchandise X (1994). Scintigraphy using amyloid P component labelled with iodine 123: A new method of evaluation of amyloidosis. Presse Med 23:348.

Hachulla E, Maulin L, Deveaux M, Facon T, Bletry O, Vanhille P, Wechsler B, Godeau P, Levesque H, Hatron PY, Huglo D, Devulder B, and Marchandise X (1996). Prospective and serial study of primary amyloidosis with serum amyloid P component scintigraphy: From diagnosis to prognosis. Am J Med 101:77–87.

Hawkins PN, Lavender JP, and Pepys MB (1990). Evaluation of systemic amyloidosis by scintigraphy with ^{123}I-labeled serum amyloid P component. N Engl J Med 323:508–513.

Hoshii Y, Kawano H, Cui D, Takeda T, Gondo T, Takahashi M, Kogishi K, Higuchi K, and Ishihara T (1997). Amyloid A protein amyloidosis induced in apolipoprotein-E-deficient mice. Am J Pathol 151:911–917.

Ikeda S, Nakazato M, Ando Y, and Sobue G (2002). Familial transthyretin-type amyloid polyneuropathy in Japan: Clinical and genetic heterogeneity. Neurology 58:1001–1007.

Ishihara T, Nagasawa T, Yokota T, Gondo T, Takahashi M, and Uchino F (1989). Amyloid protein of vessels in leptomeninges, cortices, choroid plexuses, and pituitary glands from patients with systemic amyloidosis. Hum Pathol 20:891–895.

Kaplan B, Vidal R, Kumar A, Ghiso J, and Gallo G (1999). Immunochemical microanalysis of amyloid proteins in fine-needle aspirates of abdominal fat. Am J Clin Pathol 112:403–407.

Kennelly JC, Shaw A, and Martin CN (1984). Reduction to benzidine is not necessary for the covalent binding of a benzidine azodye to rat liver DNA. Toxicology 32:315–324.

Klunk WE, Debnath ML, Koros AM, and Pettegrew JW (1998). Chrysamine-G, a lipophilic analogue of Congo red, inhibits A beta-induced toxicity in PC12 cells. Life Sci 63:1807–1814.

Klunk WE, Debnath ML, and Pettegrew JW (1994). Development of small molecule probes for the beta-amyloid protein of Alzheimer's disease. Neurobiol Aging 15:691–698.

Klunk WE, Debnath ML, and Pettegrew JW (1995). Chrysamine-G binding to Alzheimer and control brain: Autopsy study of a new amyloid probe. Neurobiol Aging 16: 541–548.

LeVine H 3rd (1993). Thioflavine T interaction with synthetic Alzheimer's disease beta-amyloid peptides: Detection of amyloid aggregation in solution. Protein Sci 2:404–410.

Masouye I (1997). Diagnostic screening of systemic amyloidosis by abdominal fat aspiration: An analysis of 100 cases. Am J Dermatopathol 19:41–45.

Matsuno H, Niikura K, and Okahata Y (2001). Direct monitoring kinetic studies of DNA polymerase reactions on a DNA-immobilized quartz-crystal microbalance. Chemistry 7:3305–3312.

Moran JK (1999). Technetium-99m-EC and other potential new agents in renal nuclear medicine. Semin Nucl Med 29:91–101.

Naiki H, Higuchi K, Hosokawa M, and Takeda T (1989). Fluorometric determination of amyloid fibrils in vitro using the fluorescent dye, thioflavin T1. Anal Biochem 177:244–249.

Okahata Y, Niikura K, Sugiura Y, Sawada M, and Morii T (1998). Kinetic studies of sequence-specific binding of GCN4-bZIP peptides to DNA strands immobilized on a 27-MHz quartz-crystal microbalance. Biochemistry 37:5666–5672.

Pepys MB, Hawkins PN, Booth DR, Vigushin DM, Tennent GA, Soutar AK, Totty N, Nguyen O, Blake CC, Terry CJ, Feest TG, Zalin AM, and Hsuan JJ (1993). Human lysozyme gene mutations cause hereditary systemic amyloidosis. Nature 362:553–557.

Puchtler H and Sweat F (1965). Congo red as a stain for fluorescence microscopy of amyloid. J Histochem Cytochem 13:693–694.

Puille M, Altland K, Linke RP, Steen-Muller MK, Klett R, Steiner D, and Bauer R (2002). ^{99m}Tc-DPD scintigraphy in transthyretin-related familial amyloidotic polyneuropathy. Eur J Nucl Med 29:376–379.

Rydh A, Suhr O, Hietala SO, Ahlstrom KR, Pepys MB, and Hawkins PN (1998). Serum amyloid P component scintigraphy in familial amyloid polyneuropathy: Regression of visceral amyloid following liver transplantation. Eur J Nucl Med 25:709–713.

Salle R, Deveaux M, Hachulla E, Descamps J, Duquesnoy B, and Marchandise X (1993). Iodine-123-labelled serum amyloid P component scintigraphy in amyloidosis. Eur J Nucl Med 20:130–137.

Saraiva MJ (2001). Transthyretin mutations in hyperthyroxinemia and amyloid diseases. Hum Mutat 17:493–503.

Sauerbrey G (1959). Verwendung von Schwingquarzed zur Wagung dunner Schichten und zur Mikrowagung. Z Phys Vio 155:206.

Schmidt ML, Schuck T, Sheridan S, Kung MP, Kung H, Zhuang ZP, Bergeron C, Lamarche JS, Skovronsky D, Giasson BI, Lee VM, and Trojanowski JQ (2001). The fluorescent Congo red derivative, (trans, trans)-1-bromo-2,5-bis-(3-hydroxycarbonyl-4-hydroxy)styrylbenzene (BSB), labels diverse beta-pleated sheet structures in postmortem human

neurodegenerative disease brains. Am J Pathol 159:937–943.

Sipe JD and Cohen AS (2000). Review: History of the amyloid fibril. J Struct Biol 130:88–98.

Skovronsky DM, Zhang B, Kung MP, Kung HF, Trojanowski JQ, and Lee VM (2000). In vivo detection of amyloid plaques in a mouse model of Alzheimer's disease. Proc Natl Acad Sci USA 97:7609–7614.

Soutar AK, Hawkins PN, Vigushin DM, Tennent GA, Booth SE, Hutton T, Nguyen O, Totty NF, Feest TG, Hsuan JJ, and Pepys MB (1992). Apolipoprotein AI mutation Arg-60 causes autosomal dominant amyloidosis. Proc Natl Acad Sci USA 89:7389–7393.

Tan SY and Pepys MB (1994). Amyloidosis. Histopathology 25:403–414.

Tan SY, Pepys MB, and Hawkins PN (1995). Treatment of amyloidosis. Am J Kidney Dis 26:267–285.

Terazaki H, Ando Y, Misumi S, Nakamura M, Ando E, Matsunaga N, Shoji S, Okuyama M, Ideta H, Nakagawa K, Ishizaki T, Ando M, and Saraiva MJ (1999). A novel compound heterozygote (FAP ATTR Arg104His/ATTR Val30Met) with high serum transthyretin (TTR) and retinol binding protein (RBP) levels. Biochem Biophys Res Commun 264:365–370.

Westermark GT, Johnson KH, and Westermark P (1999). Staining methods for identification of amyloid in tissue. Methods Enzymol 306:3–25.

Westermark GT and Westermark P (2000). Endocrine amyloid: A subject of increasing interest for the next century. Amyloid 71:19–22.

Westermark P, Benson MD, Buxbaum JN, Cohen AS, Frangione B, Ikeda S, Masters CL, Merlini G, Saraiva MJ, and Sipe JD (2002). Amyloid fibril protein nomenclature–2002. Amyloid 9:197–200.

Zenser TV, Lakshmi VM, and Davis BB (1998). N-glucuronidation of benzidine and its metabolites: Role in bladder cancer. Drug Metab Dispos 26:856–859.

Zhuang ZP, Kung MP, Hou C, Plossl K, Skovronsky D, Gur TL, Trojanowski JQ, Lee VM, and Kung HF (2001a). IBOX(2-(4'-dimethylaminophenyl)-6-iodobenzoxazole): A ligand for imaging amyloid plaques in the brain. Nucl Med Biol 28:887–894.

Zhuang ZP, Kung MP, Hou C, Skovronsky DM, Gur TL, Plossl K, Trojanowski JQ, Lee VM, and Kung HF (2001b). Radioiodinated styrylbenzenes and thioflavins as probes for amyloid aggregates. J Med Chem 44:1905–1914.

FULL PAPER *Virology*

Susceptibility of Transgenic Mice Expressing Chimeric Sheep, Bovine and Human PrP Genes to Sheep Scrapie

Altangerel GOMBOJAV[1,6], Ikuko SHIMAUCHI[1], Motohiro HORIUCHI[1], Naotaka ISHIGURO[1]*, Morikazu SHINAGAWA[1], Tetsuyuki KITAMOTO[2], Ichiro MIYOSHI[3], Shirou MOHRI[4] and Masuhiro TAKATA[5]

[1]*Laboratory of Veterinary Public Health, Obihiro University of Agriculture and Veterinary Medicine, Inada-cho, Obihiro, Hokkaido 080–8555,* [2]*Department of Neurological Sciences, Tohoku University Graduate School of Medicine,* [3]*Institute for Animal Experimentation, Tohoku University Graduate School of Medicine, Seiryou-cho, Aoba-ku, Sendai, 980–8575,* [4]*Laboratory of Biomedicine, Graduate School of Medical Science, Kyushu University, Maidashi 3–1–1 Higashi-ku, Fukuoka, 812–8582,* [5]*National Institute of Animal Health, Tsukuba, Ibaraki 305–0556, Japan and* [6]*School of Veterinary Medicine and Biotechnology, Mongolian State University of Agriculture, Ulaanbaatar 210153, Zaisan, Mongolia*

(Received 19 July 2002/Accepted 20 December 2002)

ABSTRACT. The use of Transgenic (Tg) mice expressing chimeric sheep/mouse (Sh/Mo) prion protein (PrP) and chimeric bovine/mouse (Bo/Mo) PrP genes was evaluated as a sheep scrapie model. We also investigated the potential for the transmission of sheep scrapie to a human/mouse (Hu/Mo) PrP Tg mouse line. The Sh/Mo PrP and Bo/Mo PrP Tg $Prnp^{+/+}$ or $Prnp^{0/0}$ mouse lines were inoculated intracerebrally with brain homogenates from three sheep with natural scrapie (KU, Y5 or S2). Incubation periods were slightly shorter in Sh/Mo PrP Tg $Prnp^{+/+}$, than in non-Tg mice inoculated with KU brain homogenate. In contrast, the incubation period was significantly prolonged ($p<0.05$) in Bo/Mo PrP Tg $Prnp^{+/+}$ mice inoculated with KU brain homogenate. The incubation period was significantly longer in all Tg $Prnp^{+/+}$ and $Prnp^{0/0}$, than in non-Tg mice ($p<0.01$) inoculated withY5 brain homogenate. None of the Tg $Prnp^{0/0}$ mice inoculated with S2 brain homogenate developed clinical signs and PrP^{Sc} was undetectable in their brains. These results suggested that expression of the Sh/Mo PrP or Bo/Mo PrP transgenes does not confer susceptibility to sheep prions upon mice, and thus none of the Tg mouse lines could be a suitable model of sheep scrapie. Hu/Mo PrP Tg $Prnp^{0/0}$ mice inoculated with natural and experimental scrapie or mouse prions did not develop clinical signs of scrapie and PrP^{Sc} was undetectable. These results suggested that neither sheep nor mouse strains of scrapie are highly transmissible to humans.

KEY WORDS: prion, PrP transgene, scrapie susceptibility, transgenic mouse.

J. Vet. Med. Sci. 65(3): 341–347, 2003

Transmissible spongiform encephalopathies (TSEs) including Creutzfelt-Jakob disease (CJD) in humans, scrapie in sheep and goats, and bovine spongiform encephalopathy (BSE) in cattle are characterized by spongiosis, astrocytosis and the accumulation of an abnormal protease-resistant prion protein (PrP), termed PrP^{Sc} [14].

The transmission of prions between species is often stochastic, characterized by prolonged incubation periods or even the absence of clinical signs and symptoms during the first passage in a new host. The reduced susceptibility of one species to prions derived from another is due to the "species barrier" [12]. Studies using transgenic mice expressing PrP transgenes have conclusively shown that the PrP gene is the primary determinant that controls susceptibility to foreign prions [1, 3, 8, 15–18, 20, 21]. Moreover, the incubation period of TSEs in transgenic mice is inversely proportional to the level of PrP protein produced in the host brain [13, 22].

Sheep are natural hosts for scrapie, but many restrictions affect the use of these animals to study this disease. Such limitations include the high cost of large numbers of animals, space and facilities, biohazard problems and long incubation periods. Therefore, reliable and practical animal models of sheep scrapie are required to bioassay of sheep prions.

Tg mice expressing the sheep PrP gene would be useful tools with which to bioassay sheep scrapie [13]. A host factor, provisionally called "protein X", may be involved in species-specific prion propagation [20]. In the human/mouse Tg system, the "protein X" effect can be overcome using chimeric human and mouse PrP (MHu2M PrP) [14, 20].

We developed Tg mice expressing a chimeric PrP gene (Sh/Mo or Bo/Mo PrP) and assessed their susceptibility to sheep prions with a view to using these mice as a model of sheep scrapie. We also investigated the potential transmission of sheep scrapie to the Hu/Mo PrP Tg mouse line.

MATERIALS AND METHODS

Tg mice: Four lines of Tg mice, #4, #20, #50 and #61 expressing chimeric sheep and mouse PrP genes (Sh/Mo PrP Tg $Prnp^{+/+}$), and three lines of Tg mice, #10, #43 and #46, expressing chimeric bovine and mouse PrP genes (Bo/Mo PrP Tg $Prnp^{+/+}$), which were produced by crossbreeding Tg and C57BL/6 mice, were established by Kitamoto *et al.* at Tohoku University School of Medicine (unpublished data). Figure 1 shows the organization of both chimeric PrP genes. The above mice were crossbred with knockout mice

* CORRESPONDENCE TO: ISHIGURO, N., Laboratory of Veterinary Public Health, Obihiro Univesity of Agriculture and Veterinary Medicine, Inada-cho, Obihiro, Hokkaido 080–8555, Japan.

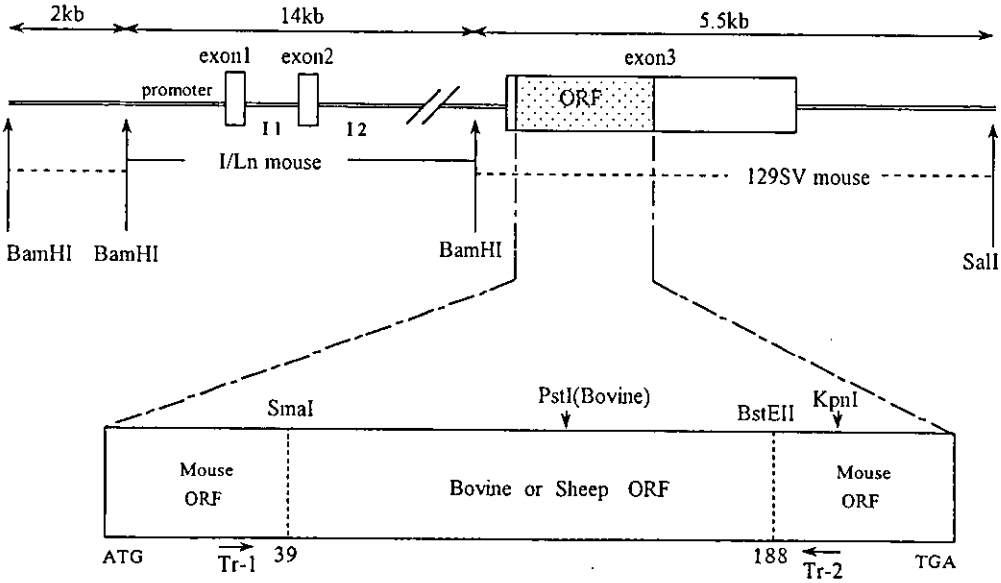

Fig. 1. Structure of chimeric PrP transgene construct. Recombinant mouse PrP gene was constructed from fragments derived from I/Ln (—) and 129SV (----) mice. Three exons indicate open boxes, and two introns indicate I1 and I2. Open reading frame (ORF) in transgenes indicated by dotted box was replaced with bovine or sheep ORF as described in Materials and Methods.

($Prnp^{-/-}$) [23], then screening these offspring for the transgene. We used Tg mice that were heterozygous for the transgene and non-transgenic littermates as controls.

Screening of transgene: Tail tissue from weaned pups was digested with 400 μl of proteinase K (150 $\mu g/ml$ in 50 mM Tris-HCl, 100 mM NaCl, 20 mM EDTA, 1% SDS, pH 8.0) at 37°C for 24 hr. Cellular DNA was extracted twice with buffered-phenol and once with chloroform:isoamyl alcohol (24:1 v/v) and precipitated with three volumes of ethanol. Mouse PrP residues 40 to 187 in the open reading frame (ORF; indicated by dotted box in Fig. 1) were replaced in the transgene with the corresponding regions of sheep PrP ORF (sheep substitutions extended from 34 to 190) or bovine PrP ORF (bovine substitutions extended from 34 to 198). The bovine ORF is a common type that contains six copies of an octarepeat sequence. The sheep ORF was derived from a sheep with the PrP amino acid polymorphisms, 136 Ala and 171 Gln. Figure 1 shows amplification of the coding region and digestion of the PrP gene. Endogenous mouse or chimeric PrP genes were differentiated by PCR using the primers, Tr-1 (5'-GCCCTCTTTGTGACTATGTGG) and Tr-2 (5'CCCCCT-TGGTGGTGGTGGTGAC). The products were digested with *Kpn* I, which cleaves the endogenous mouse PrP gene fragment at one site but not Sh/Mo PrP gene fragment, or with *Pst* I, which cleaves the Bo/Mo PrP gene fragment at one site but not the mouse PrP gene fragment.

Inoculation with sheep and mouse prions (PrP): Brains from sheep infected with natural scrapie (KU, PrP amino acid type PrP^{MARQ}/PrP^{TARQ}; Y5, PrP^{MARQ}/PrP^{MARQ} and S2, PrP^{MARQ}/PrP^{MARH}), experimental scrapie (VPH-G1, PrP^{MARQ}/PrP^{MARQ}) and the mouse adapted scrapie strain, Mo-Obihiro were sources of prions. Brain homogenates (10% w/v) in PBS were prepared by serial passage through 18-, 22- and 27-gauge needles. Mice were inoculated intracerebrally with 20 μl of 10% brain homogenate of KU, S2, VPH-G1, Mo-Obihiro and 1% brain homogenate of Y5 and S2. When death was clearly imminent, the inoculated mice were sacrificed under anesthesia. The brains were removed, cut into halves along the median line, and stored at –35°C before processing for of PrP^{Sc} detection.

Detection of PrP^{C} and PrP^{Sc}: Brain homogenate (10% w/v) from control mice was prepared in 20 mM Tris-HCl, 0.5 mM $MgCl_2$, 0.5 mM DTT, 6% Sarkosyl, 2 mM phenylmethylsulfonyl fluoride (PMSF), pH 7.5. The homogenate was stabilized for 30 min at 37°C and then separated by centrifugation at 17, 860 × g for 5 min at room temperature. The supernatant was decanted and centrifuged again at 173, 969 × g for 20 min at 20°C. The supernatant was precipitated with 10 volumes of methanol and boiled in a double-concentrated sample buffer (0.1 M Tris-HCl, 4% SDS, 2% 2-mercaptoethanol, 20% glycerol, 0.01% bromophenol blue, pH 6.8) at 100°C for 10 min.

To detect PrP^{Sc}, brains of mice infected with scrapie were minced, suspended in 6.5 volumes of 50 mM Tris-HCl, 5 mM $MgCl_2$, 2% Triton X 100, pH 7.5 and digested with DNase I (65 μg/100 mg tissue) and collagenase (650 μg/100 mg tissue) at 37°C for 3~10 hr until tissue clumps disappeared. Sarkosyl was added to a final concentration of 6.25% and the mixture was equilibrated for 30 min at 37°C before centrifugation at 17, 860 x g for 5 min at room temperature. The supernatants were digested with proteinase K

Table 1. Reactivity of anti- PrP antibodies

Antibody	Animal	Immunogen (Synthetic Peptide)	Reactivity to PrP[a]			Dilution	Reference
			Bo	Sh	Mo		
B103	Rabbit	Bo PrP residues103–121	+	+	+	1:2000	[10]
BSPX54[b]	Mouse	Bo PrP residues146–159	+	+	–	1:5	[10]
H90	Rabbit	Ha PrP residues90–104	–	–	+	1:800	[19]

a) Reactivity to respective PrP at the indicated dilution.
b) Monoclonal antibody in culture medium.
Bo, bovine; Sh, sheep; Mo, mouse; Ha, hamster (Syrian hamster).

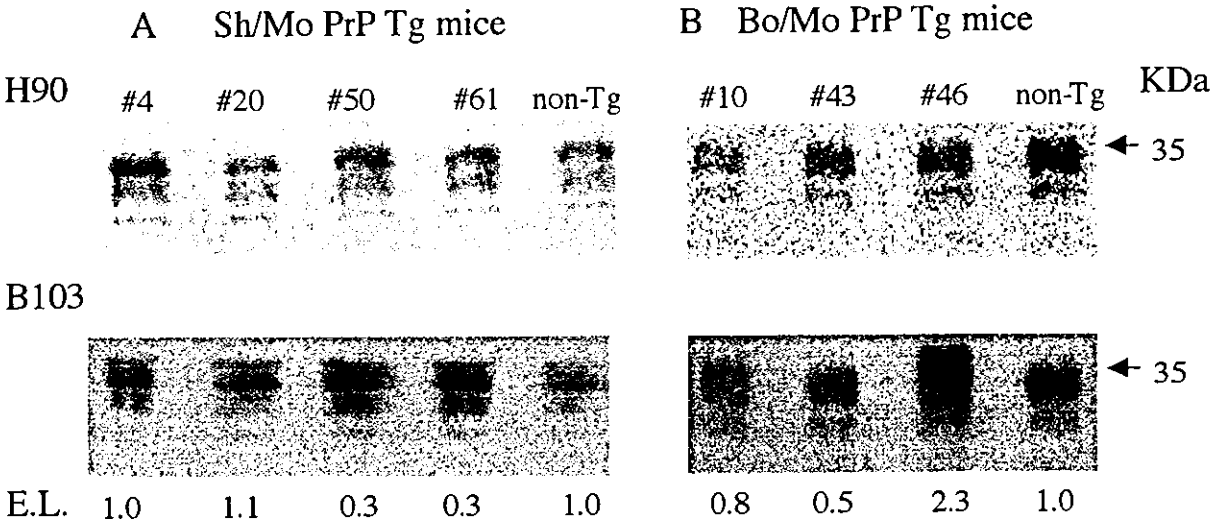

Fig. 2. Expression of PrP^C in Tg mice. Expression levels (E.L.) of PrP^C in Sh/Mo PrP Tg (A) and in Bo/Mo PrP Tg (B) mice brains estimated by relative expression of chimeric PrP gene to non-Tg PrP gene using antiserum H90 (upper panels) that reacts only with Mo PrP and antiserum B103 (lower panels) that reacts with Mo PrP, Sh PrP and Bo PrP. Membranes probed with H90 were reprobed with B103. Expression levels were estimated as described in the text. E.L.: estimated relative expression levels. Samples in A and B contained 0.5 and 0.4 mg tissue equivalent, respectively. Molecular weights of PrP^C (arrows) of 35 kDa were estimated using cytochrome *c* monomer and oligomers (Oriental Yeast, Tokyo, Japan).

(40 μg/100 mg tissue) for 2 hr at 37°C, then PMSF was added to a final concentration of 2 mM. Proteins were precipitated with nine volumes of methanol and collected by centrifugation at 17, 860 × g for 5 min at 4°C. The precipitates were dissolved in double-concentrated sample buffer at 100°C for 10 min.

Proteins were resolved by electrophoresis in 12% polyacrylamide gels containing 0.1% SDS and transferred to Hybond-PVDF membranes (Amersham, U.S.A.) using a wet blotter as described [6]. Non-specific binding was blocked using 5% skim milk, 0.2% Tween-20 in PBS on a rocking platform. PrP^{Sc}- or PrP^C- specific bands were visualized using the primary antibodies, B103, H90, or the monoclonal antibody (mAb) BSPX54 (Table 1), and the secondary antibody, horseradish peroxidase-conjugated anti-mouse or rabbit IgG (Amersham) in the ECL-Western blot detection system (Amersham). Bands were visualized and quantified using FUJIFILM LAS-1000 (FUJIFILM, Tokyo, Japan) and FUJIFILM Image Gauge (FUJIFILM, Tokyo, Japan), respectively.

RESULTS

Expression of PrP^C in Tg mice: Barriers between mouse and other species is thought to be influenced by the expression of transgene products and heterology between exogenous PrP^{Sc} and de novo PrP^C in mice. We estimated the expression of chimeric Sh/Mo PrP^C and Bo/Mo PrP^C in the brains of Tg mice by Western blotting using the antisera B103 that reacts to sheep and bovine PrP, and H90 that reacts with mouse, but not sheep and bovine PrP (Table 1 and Fig. 2). H90 antiserum detected authentic Mo PrP^C in the brains of all Tg mice (Fig. 2A and B). Authentic Mo PrP^C signals in the Tg mouse lines were quantified and normalized by comparison with the signals from non Tg mice as a standard. Signals from total PrP^C of the Tg mice in the

Table 2. Incubation periods for transmission of sheep scrapie to Tg Prnp$^{+/+}$ mice

Recipient Mouse Line	Prion strain[a)]	Affected/ inoculated[b)]	Incubation period (mean days ± SD)	p[c)]	PrP^{Sc}[d)]
Sh/Mo PrP Tg Prnp$^{+/+}$ mice					
# 50	KU	3/3	519 ± 31	0.1590	+
# 61	KU	3/3	505 ± 46	0.0837	+
Bo/Mo PrP Tg Prnp$^{+/+}$ mice					
# 10	KU	2/2	701 ± 0	0.0001	+
# 43	KU	3/3	598 ± 12	0.0116	+
# 46	KU	1/3	699	-	+
Non transgenic mice	KU	8/8	542 ± 34		+
Sh/Mo PrP Tg Prnp$^{+/+}$ mice					
# 4	Y5	8/8	512 ± 28	0.0019	+
# 20	Y5	10/10	555 ± 20	<0.001	+
# 50	Y5	3/3	493 ± 16	0.0064	+
# 61	Y5	5/5	510 ± 18	0.0003	+
Bo/Mo PrP Tg Prnp$^{+/+}$ mice					
# 10	Y5	5/5	657 ± 57	<0.001	+
# 43	Y5	6/6	598 ± 44	<0.001	+
Non transgenic mice	Y5	6/6	470 ± 5		+

a) KU, 10% brain homogenates of scrapie sheep KU; Y5, 1% brain homogenates of scrapie sheep Y5.
b) Numbers of affected/inoculated mice exclude mice dying after inoculation or developing clinical signs of scrapie.
c) P values determined by t-test.
d) All mice proteins examined by Western blotting.

same membranes reprobed with B103 antiserum were normalized by comparison with the signals from non-Tg mice in the same manner. Expression of transgene by each Tg mouse line was determined as follows. Normalized values of total PrP^{C} were divided by the respective normalized value of the authentic Mo PrP^{C} minus 1. The expression levels of the transgene in Sh/Mo PrP Tg mouse lines #4, #20, #50, and #61 were 1.0, 1.1, 0.3 and 0.3, respectively (Fig. 2A). Similarly, the levels in Bo/Mo PrP Tg mouse lines #10, #43, #46 were 0.8, 0.5, and 2.3, respectively (Fig. 2B).

Susceptibility of the Tg PrP$^{+/+}$ mice to sheep prion: Sh/Mo PrP Tg, Bo/Mo PrP Tg Prnp$^{+/+}$ and non-Tg littermate mice were inoculated with brain homogenates of sheep KU or Y5 naturally infected with scrapie as a source of sheep prion. The clinical course in affected Sh/Mo PrP and Bo/MoTg Prnp$^{+/+}$ and non-transgenic mice was characterized by progressive dysbasia, mild ataxia, whole-body tremors, ataxia, and paralysis followed by death. The incubation periods in the Sh/Mo PrP Tg Prnp$^{+/+}$ mice inoculated with KU brain homogenate seemed to be somewhat, but not significantly shorter than that in the non-Tg control. However, incubation periods were significantly prolonged in Sh/Mo PrP Tg Prnp$^{+/+}$ mice inoculated with the Y5 brain homogenate ($p<0.01$) and in Bo/MoTg Prnp$^{+/+}$ mice inoculated with KU and Y5 brain homogenates ($p<0.01$) (Table 2).

Detection of PrP^{Sc} in the brains of Tg mice: We analyzed the types of PrP^{Sc} accumulated in the brains of Sh/Mo PrP and Bo/Mo PrP Tg mice inoculated with scrapie KU homogenates using the mouse PrP specific antibodies H90 and the sheep/bovine PrP specific mAb BSPX54. Brains from the mice inoculated with sheep scrapie and the Obihiro strain [19] served as controls for Sh PrP^{Sc} and Mo PrP^{Sc} respectively (Fig. 3). Mo PrP^{Sc} was detected with H90 but not with mAb BSPX54, while Sh PrP^{Sc} was detected only with mAb BSPX54 (Fig. 3). Based on the antibody specificity, both Mo PrP^{Sc} and Sh/Mo PrP^{Sc} were detected in the brains of Sh/Mo PrP Tg mice #50 and #61 that developed symptoms of scrapie signs with KU (Fig. 3A). This indicates that the product of the transgene, Sh/Mo PrP^{C}, could be a substrate for the propagation of prions in Sh/Mo PrP Tg mice. However, less Sh/Mo PrP^{Sc} than Mo PrP^{Sc} apparently accumulated, indicating that authentic Mo PrP^{C} was dominant in Sh/Mo PrP Tg mice even though they were inoculated with sheep prions. Furthermore, Bo/Mo PrP^{Sc} in Bo/Mo PrP Tg mice inoculated with KU sheep prions was undetectable, even though Mo PrP^{Sc} was detected (Fig. 3B).

Susceptibility of the Tg PrP$^{0/0}$ mice to sheep prions: To eliminate the expression of de novo mouse PrP^{C}, Sh/Mo PrP Tg and Bo/Mo PrP Tg Prnp$^{0/0}$ mice were inoculated with brain homogenates containing the natural scrapie prions Y5 or S2. Incubation periods were significantly prolonged in

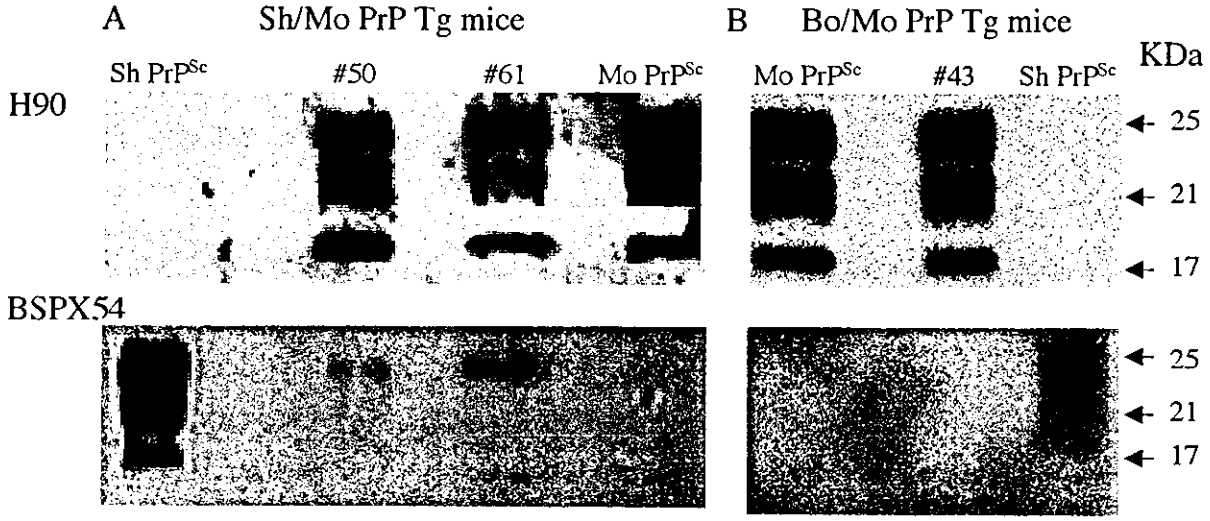

Fig. 3. Detection of PrP^{Sc} in Tg mice inoculated with sheep prions from KU. Types of PrP^{Sc} accumulated in the brain of Sh/Mo PrP Tg mice (A) and Bo/Mo PrPTg mice (B) inoculated with scrapie sheep KU brain homogenates were analyzed using mouse PrP specific antibodies H90 (upper panels) and sheep/bovine PrP specific mAb BSPX54 (lower panels). Sh PrP^{Sc}, PrP^{Sc} from sheep with scrapie; Mo PrP^{Sc}, PrP^{Sc} from ICR mice with scrapie. Molecular weights of PrP^{Sc} bands indicated by arrows estimated using cytochrome *c* monomer and oligomers (Oriental Yeast, Tokyo, Japan).

Sh/Mo PrP Tg $Prnp^{0/0}$ mouse lines inoculated with sheep prion Y5 ($p<0.001$). However, Bo/Mo PrP Tg $Prnp^{0/0}$ mouse lines inoculated with Y5 did not develop clinical signs of scrapie and PrP^{Sc} was undetectable in their brains except for one mouse (#46) in which the incubation period was 644 days. Likewise, none of the mouse lines inoculated with sheep prion S2 developed clinical signs of scrapie and PrP^{Sc} was undetectable in their brains (Table 3).

Potential transmission of sheep scrapie to Hu/Mo PrP Tg $Prnp^{0/0}$ mice: Hu/Mo PrP Tg $Prnp^{0/0}$ mice were inoculated with three natural and experimental sheep scrapie sources, namely V5, S2, VPH-G1 and Mo-Obihiro mouse scrapie prions. None developed clinical signs of scrapie and PrP^{Sc} was undetectable in their brains. In another study, when Sporadic CJD isolate was inoculated into the same mouse line, the incubation period was 156 ± 14 days [11] (Table 3). These results indicated that sheep and mouse scrapie is less transmissible to humans.

DISCUSSION

We established Tg mice (Sh/Mo PrP Tg mice) expressing the Sh/Mo chimeric PrP gene, the organization of which is similar to that of the MHu2M PrP gene, and investigated their usefulness as a model of sheep scrapie. However, the incubation periods in Sh/Mo PrP Tg mice inoculated with sheep prions were not reduced (Tables 2 and 3). Moreover, almost all accumulated PrP^{Sc} in Sh/Mo PrP Tg mice infected with scrapie were from endogenous mouse PrP^{C} (Fig. 3A). These results suggest that Sh/Mo PrP transgene expression did not facilitate mouse susceptibility to sheep prions.

Bo/Mo PrP Tg mice are more resistant to inoculated sheep prions (Table 2). Moreover, PrP^{Sc} detected in the brains of affected Tg mice was derived only from authentic mice PrP^{C}. These results indicate that Bo/Mo PrP^{C} cannot act as a substrate for the propagation of sheep prions. During the course of this study, Scott *et al.* reported that mice deficient in the authentic PrP gene but expressing MBo2M bovine/mouse chimeric PrP^{C} (MBo2M PrP is similar to Bo/Mo PrP in this study) are completely resistant to BSE prions. In contrast, Tg mice deficient in authentic PrP but expressing bovine PrP^{C} are susceptible to BSE prions [17]. Our findings are consistent with these, since Bo/Mo PrP^{C} is less competent for the propagation of PrP^{Sc} and/or prions. Tg (BoPrP) mice expressing only bovine PrP are susceptible to BSE prion and tgOv or Tg (OvPrP4) mice expressing only sheep PrP are susceptible to sheep scrapie prions [4, 17, 22].

The susceptibility of Sh/Mo PrP Tg mice to sheep prions was not enhanced despite expression of the Sh/Mo PrP transgene perhaps because of the relatively low expression levels of Sh/Mo PrP^{C} in the Tg mice. The expression level of Syrian hamster (SHa) PrP or MH2M hamster/mouse chimeric PrP and tgOv lines expressing ovine PrP in Tg mice is inversely proportional to the incubation periods after inoculation with 263K hamster prions or with PG127 and LA404 sheep scrapie prions [13, 16, 22]. In fact, an expression level of hamster PrP^{C} that was over ten-fold higher than that of mouse PrP^{C} was required to completely overcome the species barrier effect [13]. However, the expression of Sh/Mo PrP^{C} was equal to or less than that of endogenous mouse PrP^{C}. Thus, the amount of Sh/Mo PrP^{C} expression may not have been high enough to confer susceptibility.

To eliminate the influence of mouse PrP^{C}, we repeated

Table 3. Incubation periods for transmission of sheep scrapie to Tg $Prnp^{0/0}$ mice

Recipient Mouse Line	Prion strain[a]	Affected/ inoculated[b]	Incubation period or Survival time	p[c]	PrP^{Sc} [d]
Sh/Mo PrP Tg $Prnp^{0/0}$ mice					
# 20	Y5	4/11	589 ± 88	<0.001	+
# 50	Y5	11/11	722 ± 41	<0.001	+
Bo/Mo PrP Tg $Prnp^{0/0}$ mice					
# 10	Y5	0/9	61~705[e]		–
# 43	Y5	0/6	29~705[e]		–
# 46	Y5	1/5	644		+
Non transgenic mice	Y5	11/11	431 ± 25		+
Sh/Mo PrP Tg $Prnp^{0/0}$ mice					
# 20	S2	0/8	162~724[e]		–
# 50	S2	0/8	386~726[e]		–
Bo/Mo PrP Tg $Prnp^{0/0}$ mice					
# 10	S2	0/11	169~717[e]		–
# 43	S2	0/10	539~724[e]		–
Non transgenic mice	S2	0/10	658~668[e]		–
Hu/Mo PrP Tg $Prnp^{0/0}$ mice					
	Y5	0/5	132~814[e]		–
	S2	0/4	71~862[e]		–
	VPH–G1	0/4	692~927[e]		–
	Mo- Obihiro	0/3	541~697[e]		–
	Sporadic CJD	11/11	156 ± 14[f]		+

a) S2, 10% and 1% brain homogenates of sheep S2 infected with scrapie; VPH-G1, 10% brain homogenates of sheep VPH-G1 infected with scrapie; Mo-Obihiro, 10% brain homogenates of mouse Mo-Obihiro scrapie; Sporadic CJD, 10% brain homogenates of codon 129 met/met patient via i.c.

b) Numbers of affected/inoculated mice exclude mice dying after inoculation or developing clinical signs of scrapie.

c) P values determined by t-test.

d) All mice proteins examined by Western blotting.

e) Cause of death was not due to scrapie but other causes (e.g. accident, old age).

f) Data from Mohri S *et al.*, 2000.

the same experiment using Sh/Mo and Bo/Mo PrP Tg $Prnp^{0/0}$ mice (Table 3). However, the incubation periods were not reduced. In other words, authentic mouse PrP^{C} inhibition of the conversion of PrP^{Sc} may be an insignificant factor.

Sh/Mo Tg mice may have failed to overcome the species barrier because chimeric PrP is not a suitable substrate for sheep prion propagation. If the interaction between Sh/Mo PrP^{C} and inoculated sheep prion (PrP^{Sc}) was favored over that between Mo PrP^{C} and Sh PrP^{Sc}, more Sh/Mo PrP^{Sc} would have accumulated in the brains of Sh/Mo PrP Tg mice. However, we found that PrP^{Sc} in the brains of Sh/Mo Tg mice mainly consisted of Mo PrP^{Sc} (Fig. 3A). The C-terminal part of PrP might also be involved in the process of PrP^{Sc} formation [9, 17]. If so, the C-terminal amino acids in the sheep PrP gene might have been substituted by mouse PrP amino acid residues. Codons 182–230 between sheep PrP and mouse PrP differ in only six amino acid residues [7], of which some are likely to be involved in the conversion from sheep PrP^{C} to PrP^{Sc}.

The lack of susceptibility of the transgenic and non-transgenic mice lines to inoculum S2 as compared with Y5 may be related to strain characteristics (Table 3). Several scrapie strains have different effects on experimental mice [4, 22]. The pathogenicity and incubation periods of prion strains S2 and Y5 may be different in infected mice. Furthermore, sheep scrapie S2 was only heterozygous at codon 171 Gln/Arg, therefore this genetic property may influence its pathogenicity. The structures of scrapie strains may also be different.

None of the human/mouse Tg lines of mice (Hu/Mo PrP Tg $Prnp^{0/0}$) inoculated with four natural and experimental types of scrapie developed clinical signs of scrapie and their brains were negative for PrP^{Sc} (Table 3). Incubation periods for scrapie isolates in laboratory primates were significantly

longer than those associated with Kuru and CJD isolates [5]. Moreover, a French investigation of scrapie and CJD found no epidemiological relationships between the two diseases [2]. Thus, these and the present findings support the contention that scrapie is minimally or not at all transmissible to humans.

ACKNOWLEDGEMENTS. This work was partly supported by a grant from the Ministry of Health and Welfare of Japan, from the Ministry of Agriculture, Forestry and Fisheries of Japan and a Grant-in-Aid for Science Research from the Ministry of Education, Science and Culture of Japan (12460130, 12575030, 10556069).

REFERENCES

1. Bueler, H., Aguzzi, A., Sailer, A., Greiner, R.A., Autenried, P., Aguet, M.and Weissmann, C. 1993. Mice devoid of PrP are resistant to scrapie. *Cell* **73**: 1339–1347.
2. Chatelain, J., Cathala, F., Brown, P., Raharison, S., Court, L. and Gajdusek, D.C. 1981. Epidemiologic comparisons between Creutzfeldt-Jakob disease and scrapie in France during the 12-year period 1968–1979. *J. Neurol. Sci* **51**: 329–337.
3. Collinge, J., Palmer, M.S., Sidle, K.C.L., Hill, A.F., Gowland, L., Meads, J., Asante, E., Bradley, R., Doey, L.J. and Lantos, P.L. 1995. Unaltered susceptibility to BSE in transgenic mice expressing human prion protein. *Nature (Lond.)* **378**: 21–28.
4. Crozet, C., Flamant, F., Bencsik, A., Aubert, D., Samarut, J. and Baron, T. 2001. Efficient transmission of two different sheep scrapie isolates in transgenic mice expressing the ovine PrP gene. *J. Virol.* **75**: 5328–5334.
5. Gajdusek, D.C. 1977. Unconventional viruses and the origin and disappearance of Kuru. *Science* **197**: 943–960.
6. Grathwohl, K. U., Horiuchi, M., Ishiguro, N. and Shinagawa, M. 1996. Improvement of PrPSc-detection in mouse spleen early at the preclinical stage of scrapie with collagenase-completed tissue homogenization and Sarkosyl-NaCl extraction of PrPSc. *Arch. Virol.* **141**: 1863–1874.
7. Harmeyer, S., Pfaff, E. and Groschup, H. M. 1998. Synthetic peptide vaccines yield monoclonal antibodies to cellular and pathological prion proteins of ruminants. *J. Gen. Virol.* **79**: 937–945.
8. Hill, A. F., Desbruslais, M., Joiner, S., Sidle, K. C. L., Gowland, I., Collinge, J., Doey, L. J. and Lantos, P. 1997. The same prion strain causes vCJD and BSE. *Nature (Lond.)* **389**: 448–450.
9. Horiuchi, M. and Caughey, B. 1999. Specific binding of normal prion protein to the scrapie form via a localized domain initiates its conversion to the protease-resistant state. *EMBO. J* **18**: 3193–3203.
10. Horiuchi, M., Yamazaki, N., Ikeda, T., Ishiguro, N. and Shinagawa, M. 1995. A cellular form of prion protein (PrP^C) exists in many non-neuronal tissues of sheep. *J. Gen. Virol.* **76**: 2583–2587.
11. Mohri, S., Kitamoto, T., Miyoshi, I., Ishikawa, Y., Ohno, S. and Numano, J. 2000. Susceptibility for the transgenic mice expressing human/mouse chimeric prion gene to human prion (Part 3). pp. 88–93. J. Annual Report of the Slow Virus Infection Research Committee, the Ministry of Health and Welfare of Japan.
12. Pattison, I. H. 1965. Experiments with scrapie special reference to the nature of the agent and the pathology of the disease, pp. 249–257. *In*: Slow, Latent and Temperate Virus Infections. NINDB Monograph 2 (Gajdusek, D.C., Gibbs, C. J., Jr. and Alpers, M. P. eds.), U.S. Government Printing Office, Washington, D.C.
13. Prusiner, S. B., Scott, M., Foster, D., Pan, K. M., Groth, D., Mirenda, C., Torchia, M., Yang, S. L., Serban, D., Carlson, G. A., Hoppe, P. C., Westaway, D.and DeArmonds, S. J. 1990. Transgenic studies implicate interactions between homologous PrP isoforms in scrapie prion replication. *Cell* **63**: 673–686.
14. Prusiner, S. B. 1991. Molecular biology of prion diseases. *Science* **252**: 1515–1522.
15. Scott, M., Foster, D., Mirenda, C., Serban, D., Coufal, F., Walchli, M., Torchia, M., Groth, D., Carlson, G., DeArmond, S. J., Westaway, D. and Prusiner, S. B. 1989. Transgenic mice expressing hamster prion protein produce species-specific scrapie infectivity and amyloid plaques. *Cell* **59**: 847–857.
16. Scott, M., Groth, D., Foster, D., Torchia, M., Yang, SL., DeArmond, S.J. and Prusiner, S. B. 1993. Propagation of prions with artificial properties in transgenic mice expressing chimeric PrP genes. *Cell* **73**: 979–988.
17. Scott, M. R., Safar, J., Telling, G., Nguyen, O., Groth, D., Torchia, M., Koehler, R., Tremblay, P., Walther, D., Cohen, F. E., DeArmond, S. J. and Prusiner, S. B. 1997. Identification of a prion protein epitope modulating transmission of bovine spongiform encephalopathy prions to transgenic mice. *Proc. Natl. Acad. Sci. U.S.A.* **94**: 14279–14284.
18. Scott, M.R., Will, R., Ironside, J., Nguyen, H.O.B., Tremblay, P., DeArmond, S.J. and Prusiner, S.B. 1999. Compelling transgenetic evidence for transmission of bovine spongiform encephalopathy prions to humans. *Proc. Natl. Acad. Sci. U.S.A.* **96**: 15137–15142.
19. Shinagawa, M., Munekata, E., Doi, S., Takahashi, K., Goto, H. and Sato, G. 1986. Immunoreactivity of a synthetic pentadecapeptide corresponding to the N-terminal region of the scrapie prion protein. *J. Gen. Virol.* **67**: 1745–1750 .
20. Telling, G. C., Scott, M., Mastrianni, J., Gabizon, R., Torchia, M., Cohen, F. E., DeArmond, S. J. and Prusiner, S. B. 1995. Prion propagation in mice expressing human and chimeric PrP transgenes implicates the interaction of cellular PrP with another protein. *Cell* **83**: 79–90.
21. Telling, G. C., Scott, M., Hsiao, K. K., Foster, D., Yang, S. L., Torchia, M., Sidle, K. C., Collinge, J., DeArmond, S. J. and Prusiner, S. B. 1994. Transmission of Creutzfeldt-Jakob disease from humans to transgenic mice expressing chimeric human-mouse prion protein. *Proc. Natl. Acad. Sci. U.S.A.* **91**: 9936–9940.
22. Vilotte, J.L., Soulier, S., Essalmani, R., Stinnakre, M.G., Vaiman, D., Lepourry, L., Silva, J.C.D., Besnard, N., Davson, M., Buschmann, A., Groschup, M., Petit, S., Madelaine, M.F., Rakatobe, S., Dur, A.L., Vilette, D. and Laude, H. 2001. Markedly increased susceptibility to natural sheep scrapie of transgenic mice expressing ovine PrP. *J. Virol.* **75**: 5977–5984.
23. Yokoyama, T., Kimura, M. K., Ushiki, Y., Yamada, S., Morooka, A., Nakashiba, T., Sassa, T. and Itohara, S. 2001. *In vivo* conversion of cellular prion protein to pathogenic isoforms, as monitored by conformation-specific antibodies. *J. Biol. Chem.* **276**: 11265–11271.